

THE OHIO STATE UNIVERSITY

## SCARLET II DESIGN TEAM

HYPERSONIC RECONNAISSANCE AIRCRAFT

Spring Quarter 1992

(NASA-CR-192049) HYPERSONIC  
RECONNAISSANCE AIRCRAFT Scarlet 2  
design team (Ohio State Univ.)  
80 p

N93-17804

Unclass

G3/05 0141632

### TEAM MEMBERS

Tim Bulk

David Chiarini

Kevin Hill

Bob Kunszt

Chris Odgen

Bon Truong

## ABSTRACT

This report is for a conceptual design of a hypersonic reconnaissance aircraft for the U.S.Navy. After eighteen weeks of work, a waverider design powered by two augmented turbofans was chosen. The aircraft has been designed to be based on an aircraft carrier and to cruise 6,000 nautical miles at Mach 4;80,000 feet and above. As a result the size of the aircraft was only allowed to have a length of eighty feet, fifty-two feet in wingspan and roughly 2,300 square feet in planform area. Since this is a mainly cruise aircraft, sixty percent of its 100,000 pound take-off weight is JP fuel. At cruise, the highest temperature that it will be encounter is roughly 1,100 degrees Fahrenheit, which can be handled through the used of a passive cooling system.

## TABLE OF CONTENTS

	PAGE
Abstract	ii
List of Figures	v
Sections	
Introduction	1
Aerodynamics	
Design History	4
Waverider Aerodynamics	15
Subsonic Aerodynamics	16
Transonic Aerodynamics	19
Supersonic Aerodynamics	22
Waverider Changes	24
Mission Profile	26
Trajectory Approach	26
Take-off and Climb Characteristics	27
Cruise	31
Descent and Landing	32
Map Profile	32
Propulsion System	36
Engine Inlets	43
Weight Analysis	46
Inboard Planform	49
Thermal Protection Systems	53
Stability and Control	59

	PAGE
Landing Gear	63
Cost Analysis	68
Summary	71
Conclusion	72
References	73

## LIST OF FIGURES

FIGURE	PAGE
1. Initial Design	5
2. Aircraft shape trade study	8
3. Aircraft trade study	8
4. Aircraft performance trade study	10
5. Second design iteration vehicle	11
6. Navy catapult limitations	12
7. Finalized configuration	13
8. Power law and cone law waverider comparison	14
9. Power law and cone law volume comparison	14
10. $C_l$ versus angle of attack subsonic	17
11. $C_l$ versus angle of attack during flight regime	17
12. Drag polar flight regime	20
13. $L/D$ versus Mach number flight regime	21
14. Drag component build-up	23
15. Dynamic pressure trajectory	29
16. Rate of climb versus Mach number	29
17. Weight versus time	30
18. Altitude versus range	30
19. $L/D$ versus Mach number for mission profile	34
20. Geographical mission profile	35
21. Fuel volume versus range	38
22. SFC versus specific thrust	38
23. Thrust versus Mach number	41
24. Fuel consumption per Mach number	41
25. Final engine dimensions	42
26. Inlet design	45

# LIST OF FIGURES CONTINUED

FIGURE	PAGE
27. Take-off weight pie chart	48
28. Structural pie chart	48
29. Volume pie chart	51
30. Planform view	52
31. Passive thermal materials	55
32. Temperature contours	56
33. Temperature distribution across flight regime	58
34. Stability derivatives	61
35. Longitudinal state equations	61
36. $C_m/C_l$ versus Mach number	62
37. Simple stability control loop	62
38. U.S. Navy landing gear requirements	65
39. Main landing gear	66
40. Rear landing gear	66
41. Gear specifications	67
42. Cost breakdown	69
43. Operational costs	69

## INTRODUCTION

The major design requirements were for a sea launched aircraft to cruise between Mach 4 and 7 at 80,000 feet, and and capable of a 6,000 nautical mile range. This presented an extremely difficult challenge since no current sea launched aircraft has a range of 6,000 nautical miles.

Since no particular launch platform was specified, two options were proposed. One was to launch from a ballistic missile submarine, such as the present day Ohio class submarine. The other was to launch from an aircraft carrier. The idea of launching from a submarine came about because ballistic missiles were the only sea launched vehicle that have a 6,000 nautical mile range. At first this idea seemed plausible because many aspects of a missile were similar to that of an aircraft that was to be designed. For example, missiles do have payloads, it is basically a flying fuel tank, and heavy engines were required to fly it. However, having consulted with navy personnel, they explained that there were too many restrictions for a submarine launch. The complexity of a folding cruise missile/aircraft inside a missile tube and revealing the submarine's location any time an aircraft is launched did not seem credible.

As a result, the second option was chosen. Launching from a carrier allowed a larger aircraft, namely a length increased from forty-four feet in a submarine to eighty feet on an aircraft carrier. This option does have its own size restriction. A carrier based aircraft has to be no more than

eighty feet in length, seventy-five feet in wingspan, less than 100,000 pounds for take-off weight and 80,000 pounds for empty weight.

Using the size limitation and 100,000 pounds as a design goal, trade studies were performed to determine an aircraft configuration that could meet and come as close to meeting the project requirements that were first set forth. Starting with aerodynamics, the aircraft configurations that were included in the trade studies were: the derivatives X-24C and FDL-7mc from AIREZ software, the waverider from MAXWARP (Maryland Axisymmetrical Waverider Program), and other configurations that were studied in several NASA technical reports. From this trade study, a waverider was determined to be the best choice because of its high lift to drag ratio at 8.26, which translates into an excellent cruise aircraft.

Since this aircraft is designed to take-off and land on an aircraft carrier, powered flight was required for the entire mission. Knowing this there was only two type of engines that were considered, augmented turbofans and augmented turbojets. The tie breaking decision was that our engines had to be as fuel efficient as possible because the volume for fuel was limited. When considering the inefficiency of usable volume in a waverider and fuel handling safety, JP fuel was an obvious choice for fuel.

After the final aircraft configuration was chosen, a trajectory analysis was performed to confirm that this aircraft could cruise for 6,000 nautical miles at Mach 4. A heating effect analysis was also performed during cruise.



The hottest temperature was found to be 1,100 degrees Fahrenheit, which according to today's material technology would allow for the use of a passive thermal protection system. A passive thermal protection system would in turn save weight and help to meet the 100,000 pound take-off weight requirement.

## AERODYNAMIC DESIGN HISTORY

The initial phase in the design process of the hypersonic navy aircraft was to establish the limitations placed on carrier aircraft. These limitations would be the starting point for our initial design estimates. From information obtained from the Navy, and various other aerodynamic sources, we were able to choose the initial estimates for weight, wingspan, and length. The next step in the preliminary design process was to evaluate various hypersonic vehicles to determine the best aircraft to fit the mission profile. Once the vehicle configuration was chosen an in-depth aerodynamic profile was completed on the vehicle.

The limitations placed on a naval carrier aircraft are: maximum wingspan of 75 ft., maximum length of 80 ft., and maximum empty weight of 80,000 pounds (due to maximum elevator load). With these limitations the initial guess for an aircraft size was 80 ft. by 60 ft..

The initial design configuration was a vehicle that met all the take-off and cruise requirements. This was done so that a rough estimate could be made on the type of vehicle that was going to be designed. The aircraft in figure 1 shows the largest wingspan and length possible for a naval aircraft. The assumptions that were made on the first design included the vehicle using the entire length of the aircraft carrier for take-off. This proved unfeasible since the catapult does not extend the entire length of the carrier.

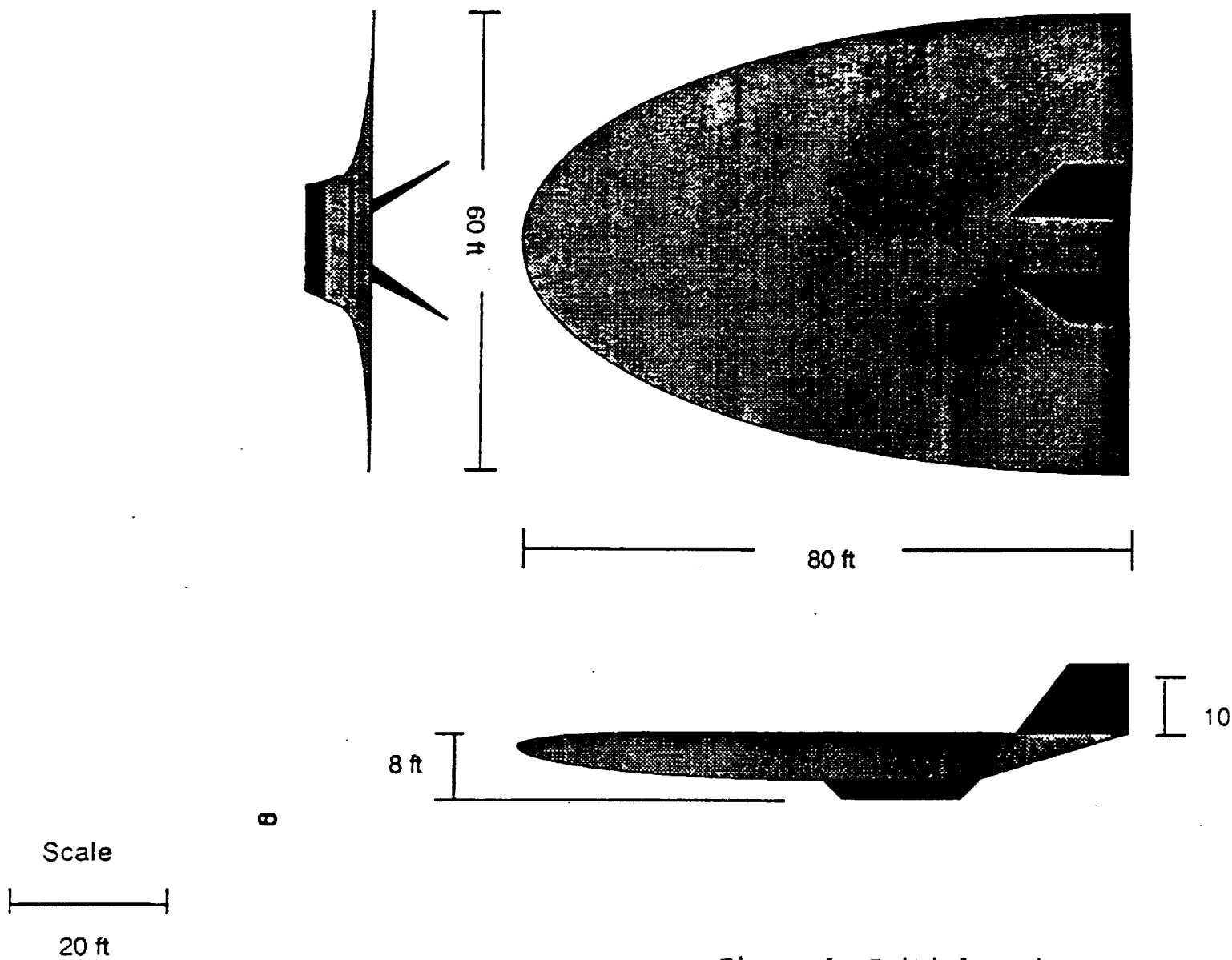


Figure 1. Initial Design

Therefore, an aircraft comparison was needed to choose the best vehicle to fit all the design conditions.

In order to design an efficient cruise vehicle it was necessary to analyze three categories of hypersonic vehicles. The first were various hypersonic gliders which have been wind tunnel tested by NASA. The second variety were several types of waveriders, followed by various hypersonic vehicles designed using AIREZ<sup>1</sup> software.

The initial phase of the design comparison included a literature research into previously designed hypersonic vehicles. Using several NASA technical journals a variety of shapes and configurations were found. Included in the journals were lift to drag versus Mach number graphs and coefficient of lift and drag data. This was beneficial in choosing the best design configuration for a cruise vehicle.

Since the type of vehicle we were designing was unique and had never been developed before, shapes and sizes of similar vehicles were limited. Therefore, it was necessary to find a preliminary design program to evaluate a variety of hypersonic vehicles to fit the Navy requirements. The program used was the AIREZ software.

The AIREZ code was developed by Bud Zeck at Boeing Aircraft. This software is a preliminary hypersonic design code which analyzes various hypersonic vehicles. The designs are entered in as data, which include: wingspan, fuselage length, and airfoil type. The program then analyzes the vehicle through an ascent trajectory, and prints out various

lift and drag coefficients for different angles of attack. With this program five different vehicles, each a variation of the FDL-7mc and the X-24C, were designed and analyzed. The second program used was the MAXWARP<sup>2</sup> waverider code. This code designs a base waverider with a high aerodynamic efficiency based on the flow field properties at a given Mach number and altitude. Other inputs include the length and width of the vehicle and the choice of power law or cone generated waveriders. Due to the propulsion and weight requirements, Mach 4 at 80,000 ft. was chosen. For the second design iteration an aircraft length of 80 ft. was chosen to make use of the limitations placed on the vehicle. The aircraft produced by the program had a wingspan of 63.5 feet and a planform area of 2340 ft<sup>2</sup>. The volume of the aircraft was 6035 ft<sup>3</sup>, and attained a maximum lift to drag of 8.26 .

Several graphs were made to show the comparison of the various designs. The graphs presented show the lift to drag versus Mach number and lift to drag versus coefficient of lift. Observing figure 2, the aircraft shape comparison graph shows various hypersonic models compared to the waverider. At a cruise speed of Mach 4, the graph shows that the waverider vehicle was producing a lift to drag ratio of 8.2, while the flat top, symmetric, and flat bottom models only produced lift to drag ratio of 4.3 to 5.0 . It should be noted that all the shapes were tested without fins nor engine housing.

## AIRCRAFT SHAPE COMPARISON

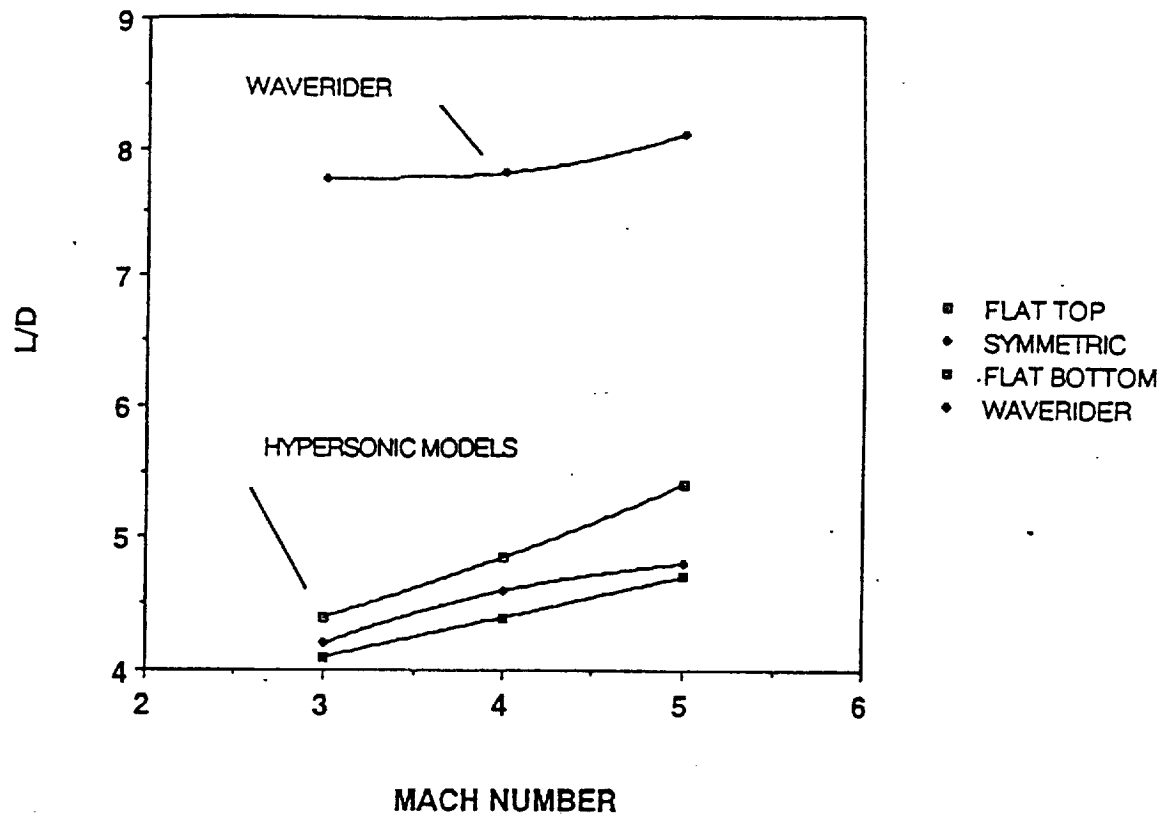


Figure 2. Aircraft shape trade study

## AIRCRAFT COMPARISON

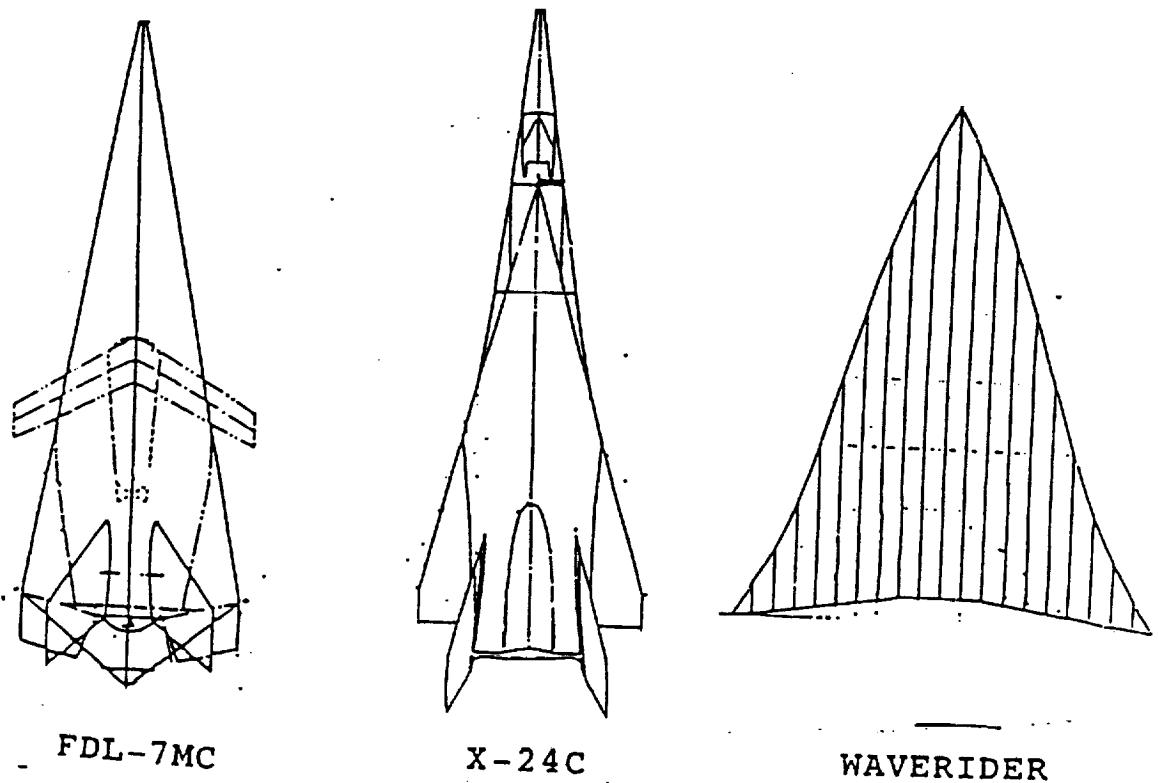


Figure 3. Aircraft trade study

Figure 3 shows the top view of the AIREZ designed vehicles and the waverider. In figure 4 the aircraft comparison between the AIREZ vehicles and the waverider aircraft is shown. Choosing the data from the best two AIREZ designs and comparing them with the waverider showed that the waverider produced a larger lift to drag ratio than the designed vehicles. Thus, because of the large lift to drag ratios produced at Mach 4 the waverider was chosen for the design.

The vehicle shown in figure 5 shows the second aircraft that was considered. This aircraft also met the cruise and size requirements but did not meet the take-off requirements. This was due to the aircraft's weight which was estimated at 155,000 lbs. This weight exceeded the Navy's catapult capabilities shown in figure 6. Thus, a third design iteration was needed to reduce the size and weight of the aircraft.

The vehicle in figure 7 was the finalized hypersonic configuration. The size and weight was reduced by completing another trade study between length, volume, and lift to drag ratio. This work was completed using the Maxwarp software. Figures 8 and 9 show the comparison that was completed between the power law and cone flow waverider configurations. The optimum length chosen was 70 ft. with a L/D of 7.3 . The finalized volume was 5516 cubic feet.

The final configuration met all the size and weight requirements specified by the Navy, and it also met all the design requirements. It is powered by two augmented turbofan

# AIRCRAFT COMPARISON AT MACH 4

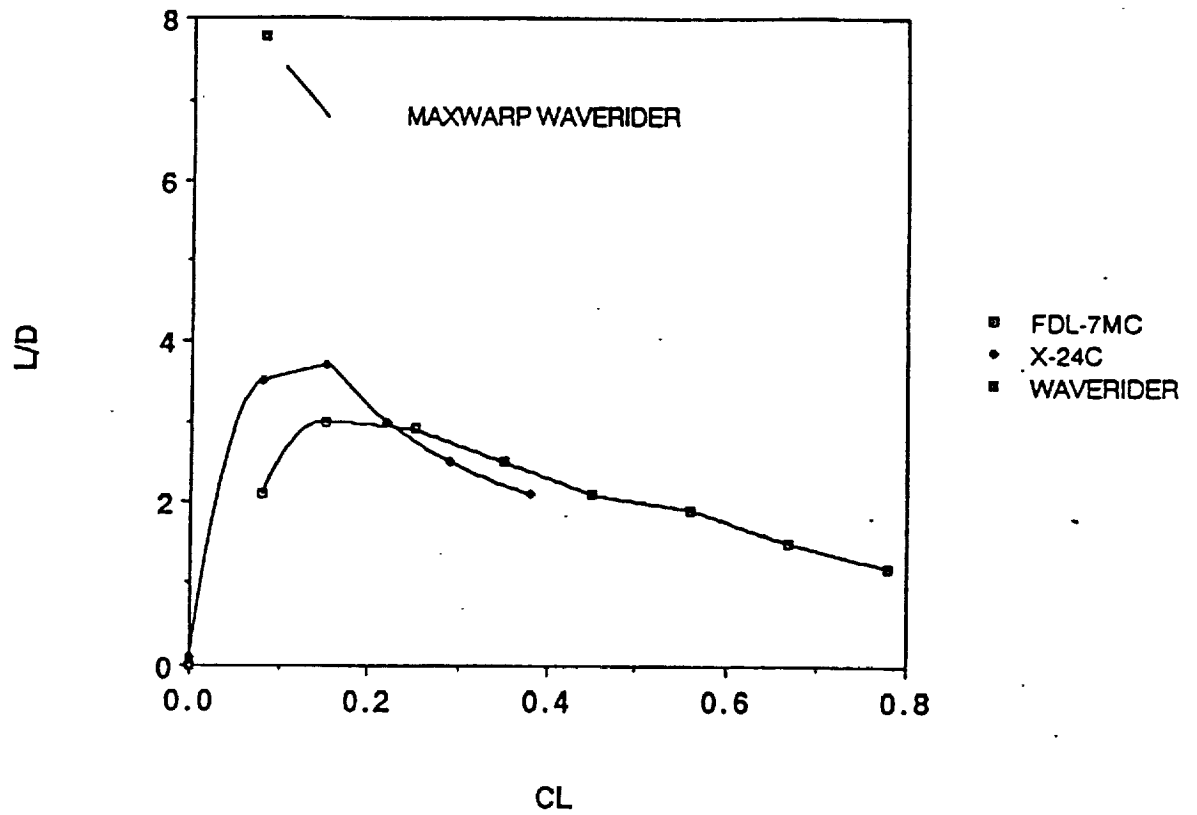
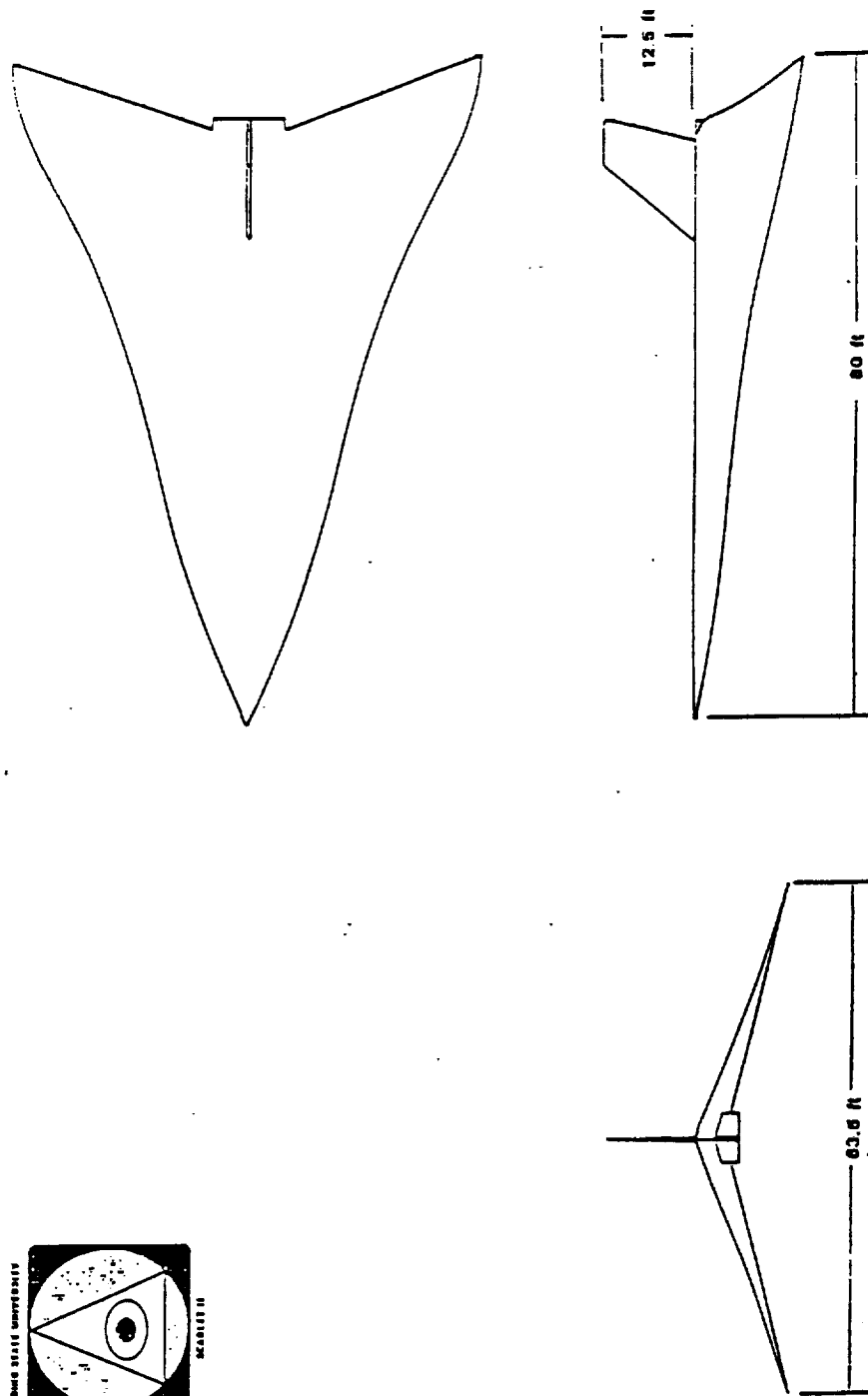
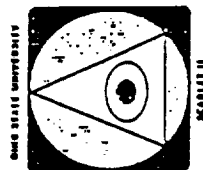


Figure 4. Aircraft performance trade study





3-VIEW HYPERSONIC UNMANNED RECONNAISSANCE WAVERIDER

SCALE 1" = 20 ft

Figure 5. Second design iteration vehicle

## EFFECT OF TAKE-OFF WEIGHT ON CATAPULT

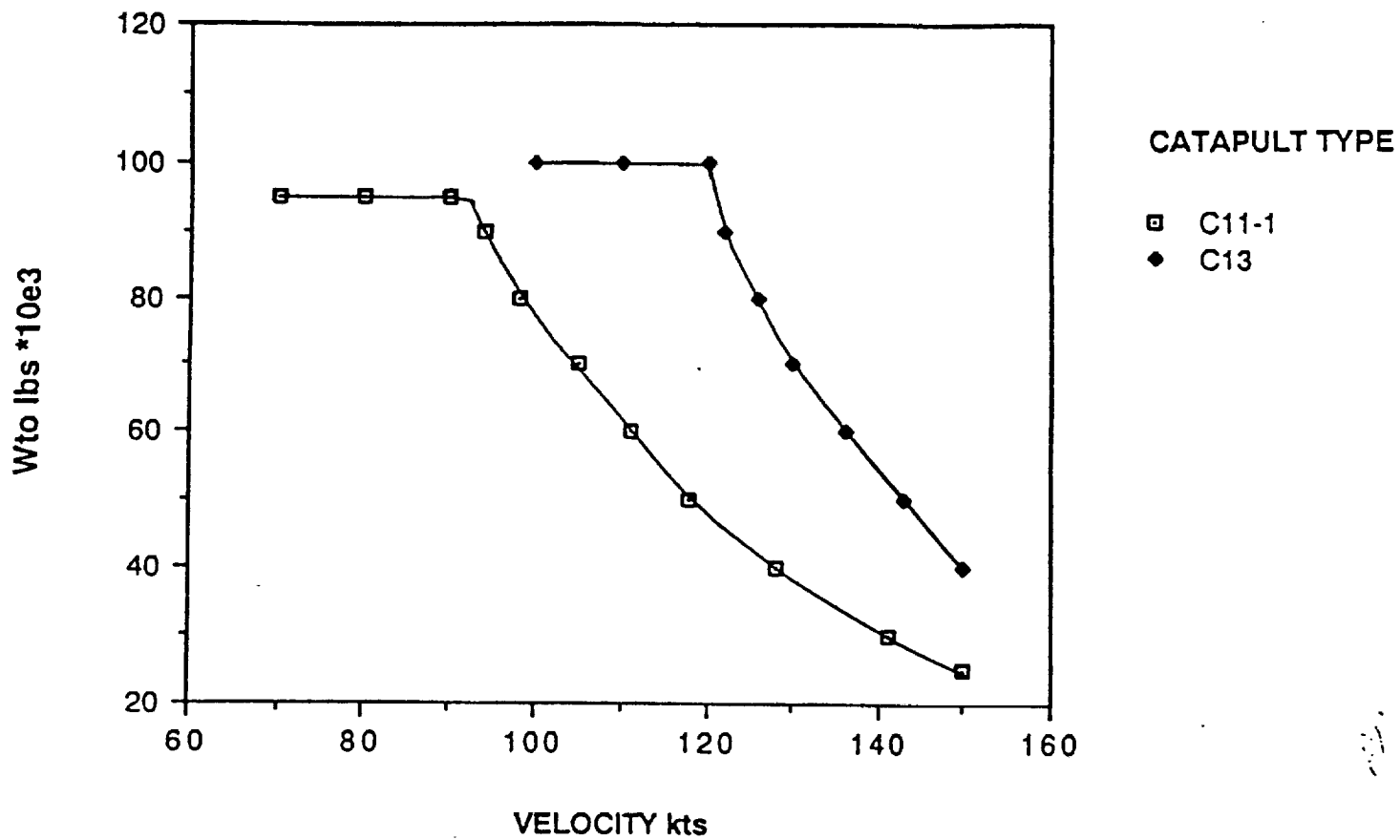


Figure 6. Navy catapult limitations

SCARLET II  
HYPERSONIC RECONNAISSANCE  
AIRCRAFT

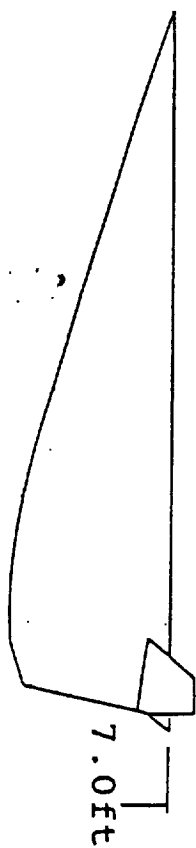
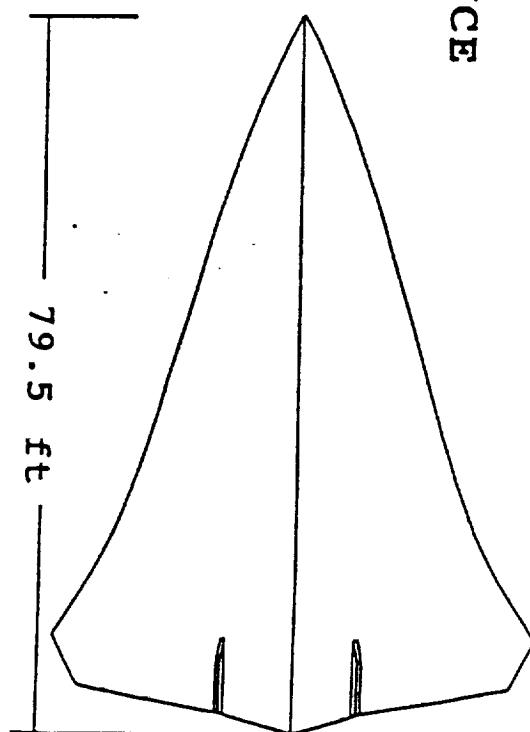
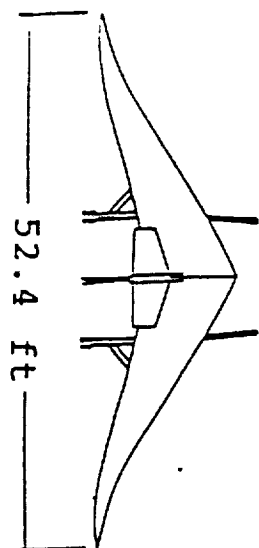


Figure 7. Finalized configuration

## L/D COMPARISON BETWEEN POWER LAW AND CONE FLOW

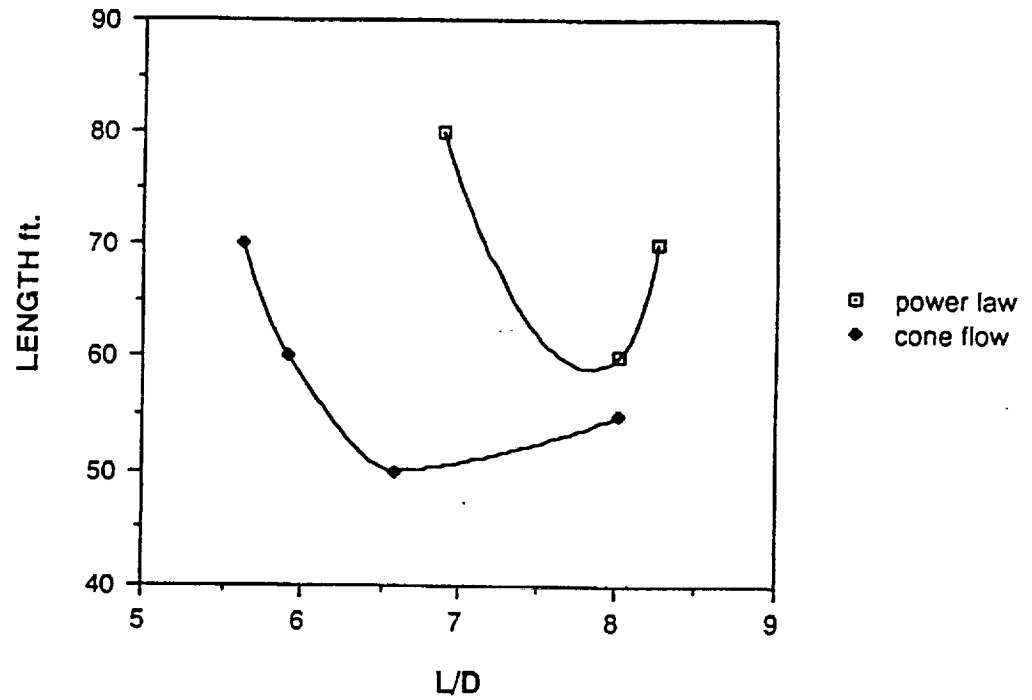


Figure 8. Power law and cone law waverider comparison

## VOLUME COMPARISON

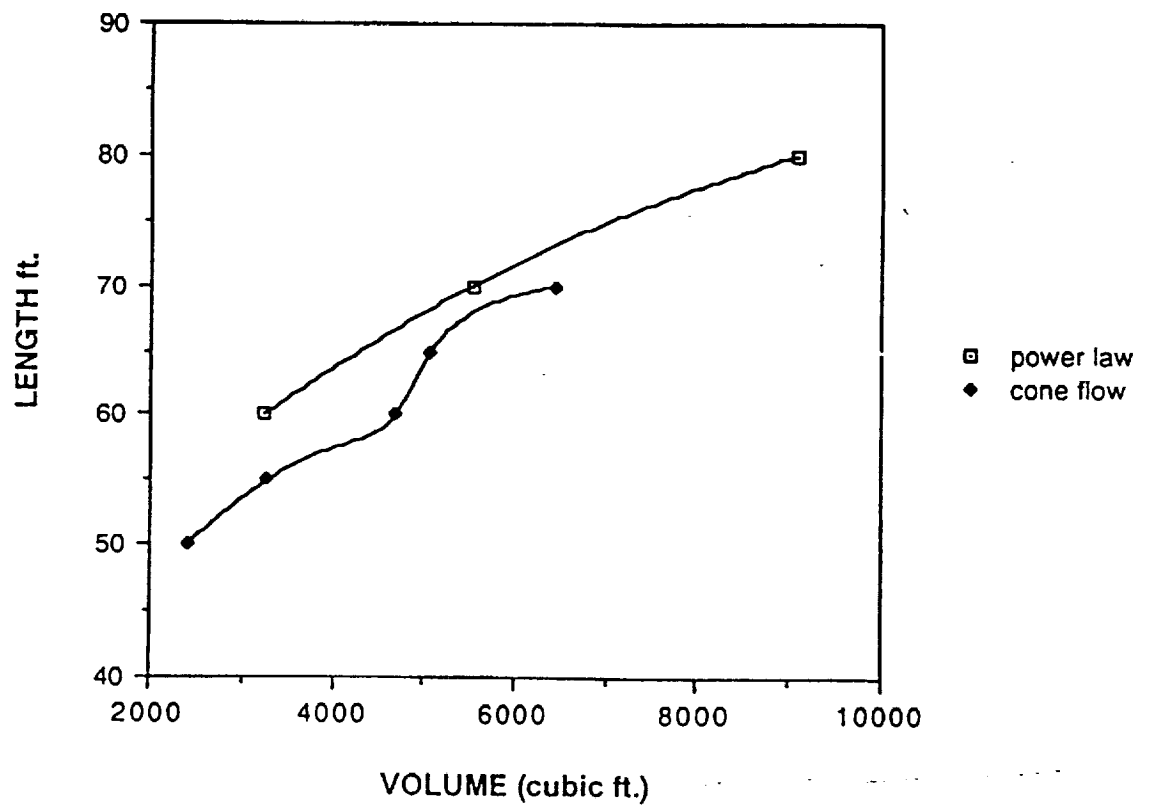


Figure 9. Power law and cone law volume comparison

engines and has a maximum take-off weight of 100,000 lbs.

### WAVERIDER AERODYNAMICS

The waverider aircraft configuration is put together from the known solutions of the inviscid flow equations.<sup>3</sup> The flow is determined from oblique shock relations and formulas, and then the shape is fitted to that flowfield. That is why the waverider is considered an inversely designed vehicle. The term 'waverider' is derived from the phenomenon of the leading edges of the vehicle riding on the surface of the planar shock wave.<sup>4</sup> These types of aircraft have good design point characteristics, but their off-design characteristics tend to be less favorable.

The good design characteristic of the waverider design is the large lift to drag ratio. The low drag is due to the low amount of pressure drag on the lower panels and the leading edges. This is due to the planar shock along the leading edges. The streamwise panels at its design point produce no pressure drag.

The large lift is due to factors, the first is because since the waverider rides on the shock wave high pressure is applied to the bottom surface of the waverider. Thus, there is high lift at high Mach numbers. The second reason is because of the great pressure differences between the top and bottom of the vehicle.

## SUBSONIC AERODYNAMICS

The design presented two aerodynamically challenging cases: cruise and takeoff. It was known from other studies that the waverider did not have good subsonic flight characteristics. Since the waverider is basically a point design vehicle for cruise, the off-design characteristics needed to be analyzed. In order to model the waverider in the subsonic flight regime, it was necessary to make some initial assumptions. The waverider is essentially a delta wing configuration where the leading edge is designed to lie along the shock produced at supersonic speeds. The cross-sectional area increases aft of the nose and is greatest at the base. For this reason, the waverider would be modeled as a flat plate delta wing of finite thickness with a sharp leading edge. The waverider chosen had an aspect ratio of 1.5 and a leading edge sweep of 69.5 degrees.

Basic research was conducted on flat plate delta wings in order to obtain some useful empirical data. From reference 1, computed and measured lift and drag data were obtained for a 74 degree delta wing at a free stream Mach number of 0.3 . The data provided a graph of lift coefficient versus angle of attack (figure 10 & 11). The lift curve slope was 0.04 per degree with a stall angle of about 37 degrees. This data was very crucial for take-off analysis.

At take-off, a velocity of 130 knots could be obtained using the catapult and having a wind over the deck of 20

# CL versus AOA

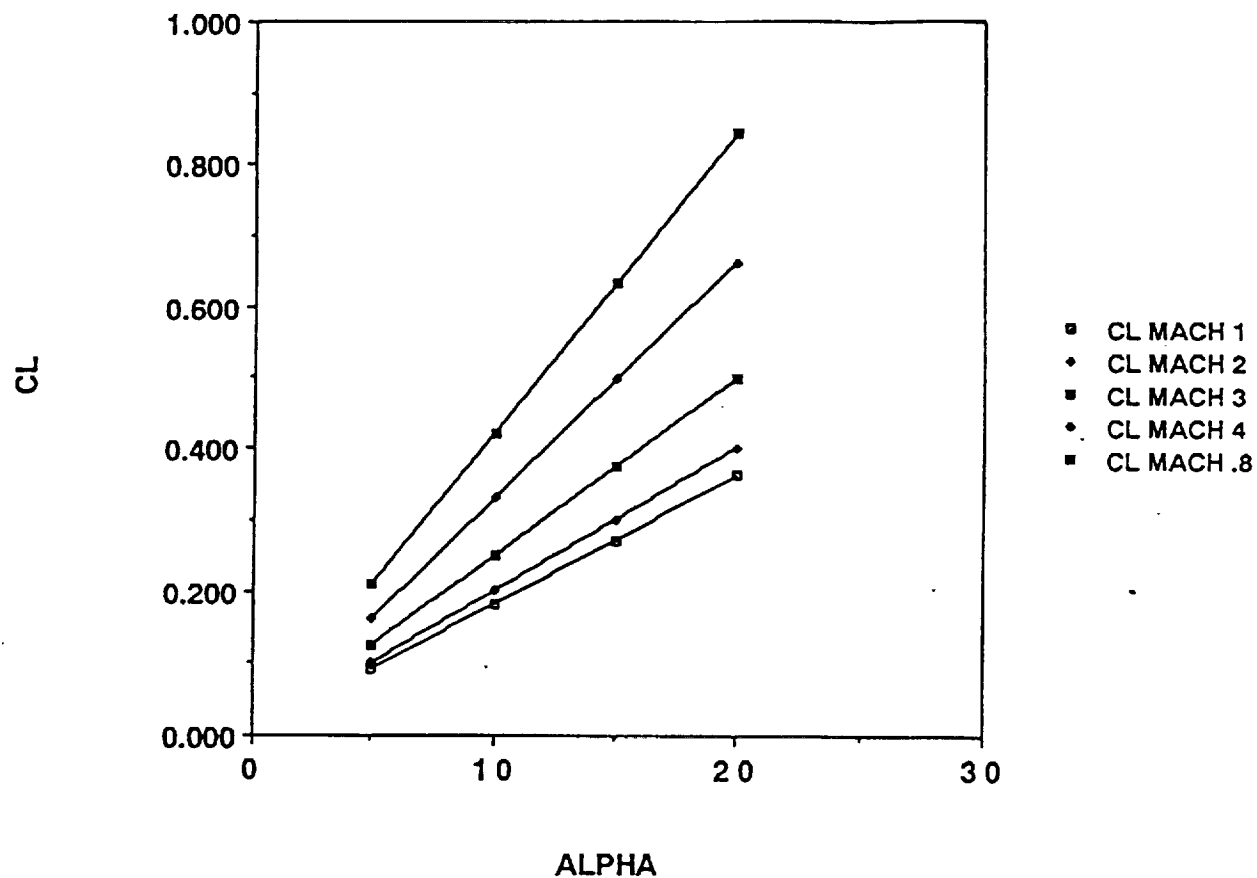
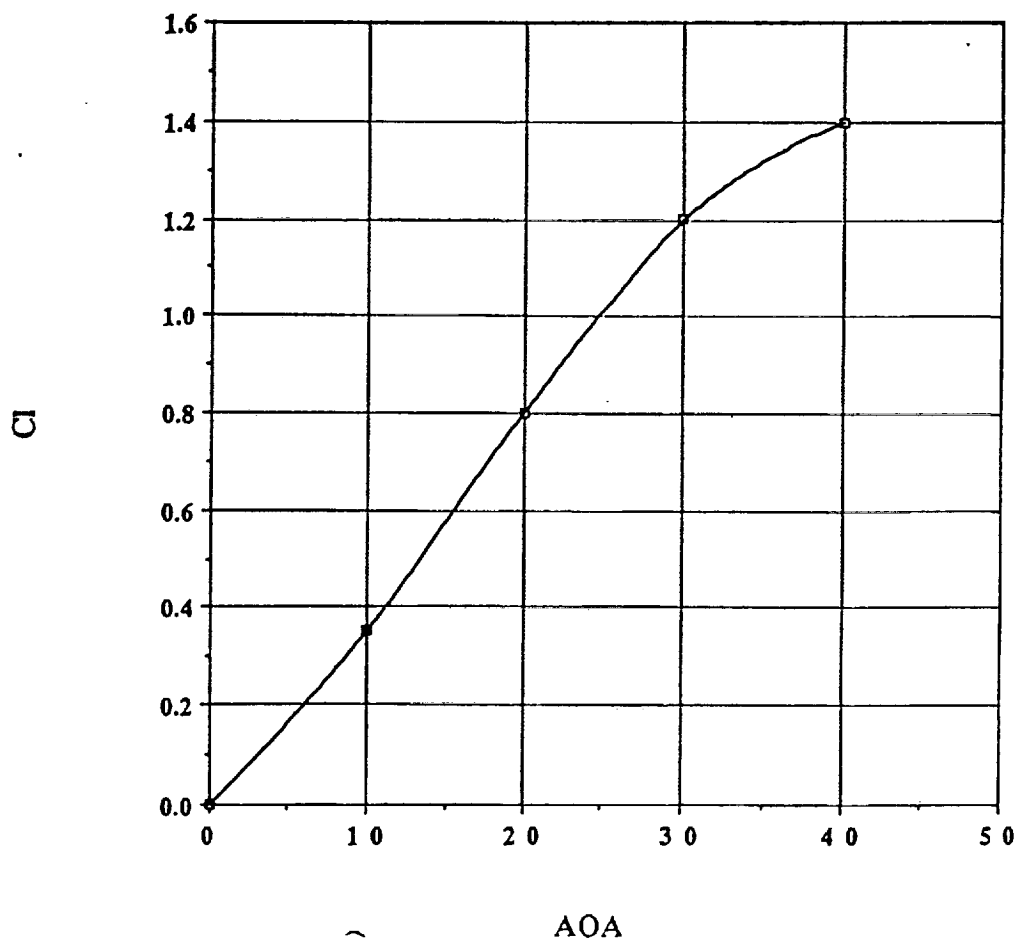


Figure 11. Cl versus angle of attack during flight regime

## Cl v. AOA (Subsonic)



ORIGINAL PAGE IS  
OF POOR QUALITY

Figure 10. Cl versus angle of attack subsonic

knots. Because of the wing loading of 43.5 lbs/ft<sup>2</sup> a lift coefficient of 1.4 was needed at take-off. This could be achieved through the use of flaps deflected at 10°. The angle of attack at take-off needed to be 14°. This cannot be achieved during catapult launch due to the front landing gear. This is achieved immediately after the catapult hitch is released and the aircraft can be rotated. Since the center of gravity for this aircraft is 67% from the front, the nose of the aircraft is easily rotated after it is off the deck of the carrier. The stall speed at take-off for this aircraft is 97.3 knots.

To model the aerodynamic characteristics, a program was written (see appendix) with the delta wing assumptions. Using reference 3, the parasite drag consisted of 70% skin friction and 30% pressure drag. The lift curve slope was based upon the aspect ratio and leading edge sweep in the subsonic region. The skin friction took into account the wetted area of the base vehicle, the tails and the engine box. Since the aircraft must take-off at a high lift coefficient, the lift to drag ratio was low. However, once the aircraft picks up speed the lift to drag ratio improves as the coefficient of lift moves closer to maximum lift-to-drag.



## TRANSONIC AERODYNAMICS

The transonic flow regime was difficult to model since there is no real theoretical method to apply. Subsonic and supersonic theory breakdown in the transonic region. Most of the data would be taken from empirical methods. References 2,3, and 4 provided some experimental data that could be used to determine the parasite drag increase.

When the free stream Mach number exceeds the drag divergence Mach number, the parasite drag increases rapidly due to the formation of shock waves. Methods used to reduce the peak drag coefficient include sweeping the wings and decreasing the aspect ratio. The waverider configuration included these characteristics; therefore, it is probable that the thrust pinch could be beaten by making sure the drag does not get extremely high in this region. Historically, the parasite drag coefficient may double or triple due to the wave drag associated with the pressures behind the shocks.

Drag polars were introduced with the program used for the mission profile (figure 12). It was decided that the parasite drag in the transonic region would double that at Mach number of .8 for the program. The drag polars were calculated using the drag polar equations, the coefficient of lift curve slopes to calculate lift coefficients, the induced lift factor, and the parasite drag build-up.

The drag polars helped in obtaining the graph of lift to drag versus Mach number for the mission profile (figure 13). This graph shows that the lift to drag starts very low due to

# DRAG POLAR

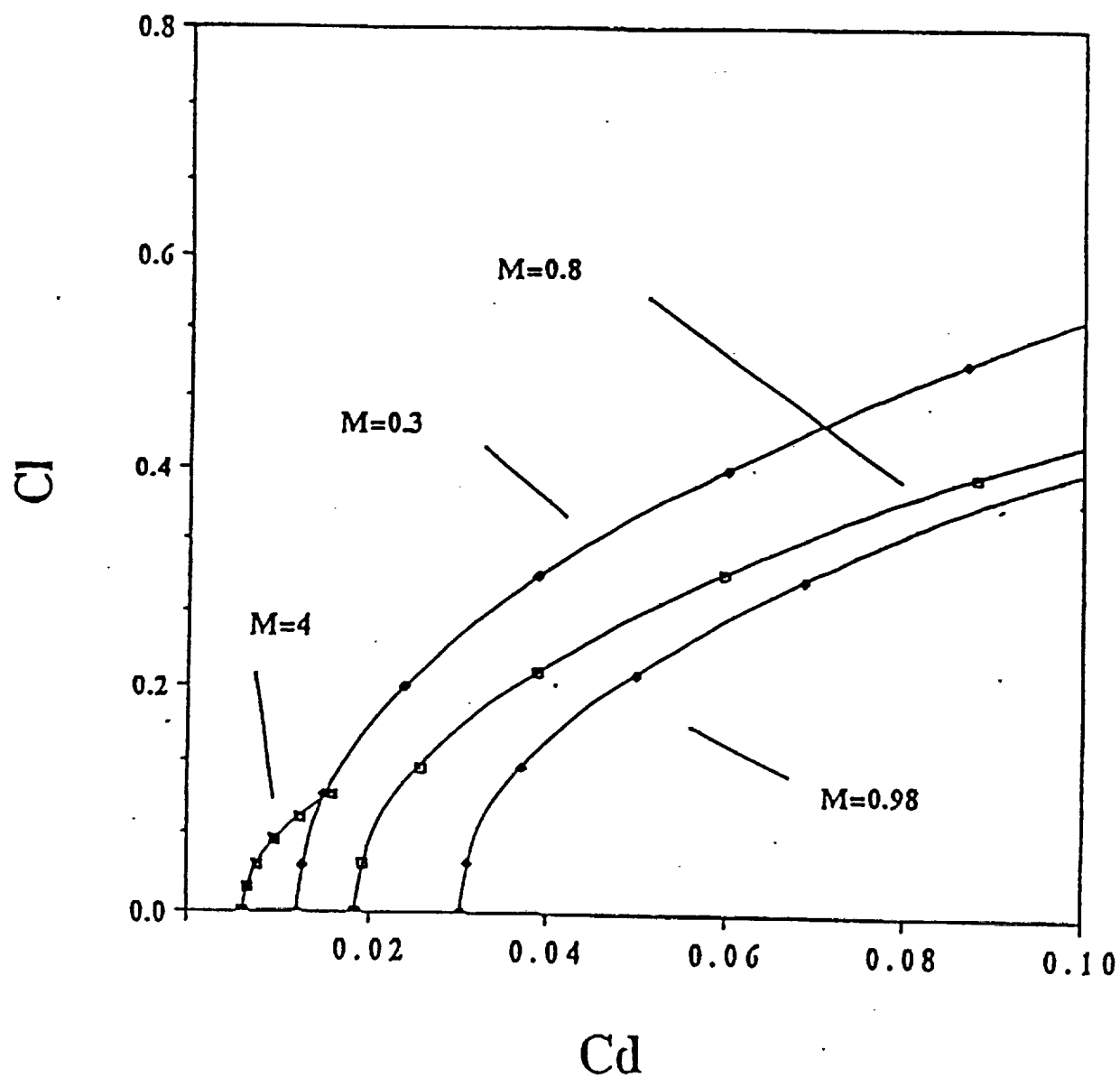


Figure 12. Drag polar flight regime

## L/D v. Mach for Mission

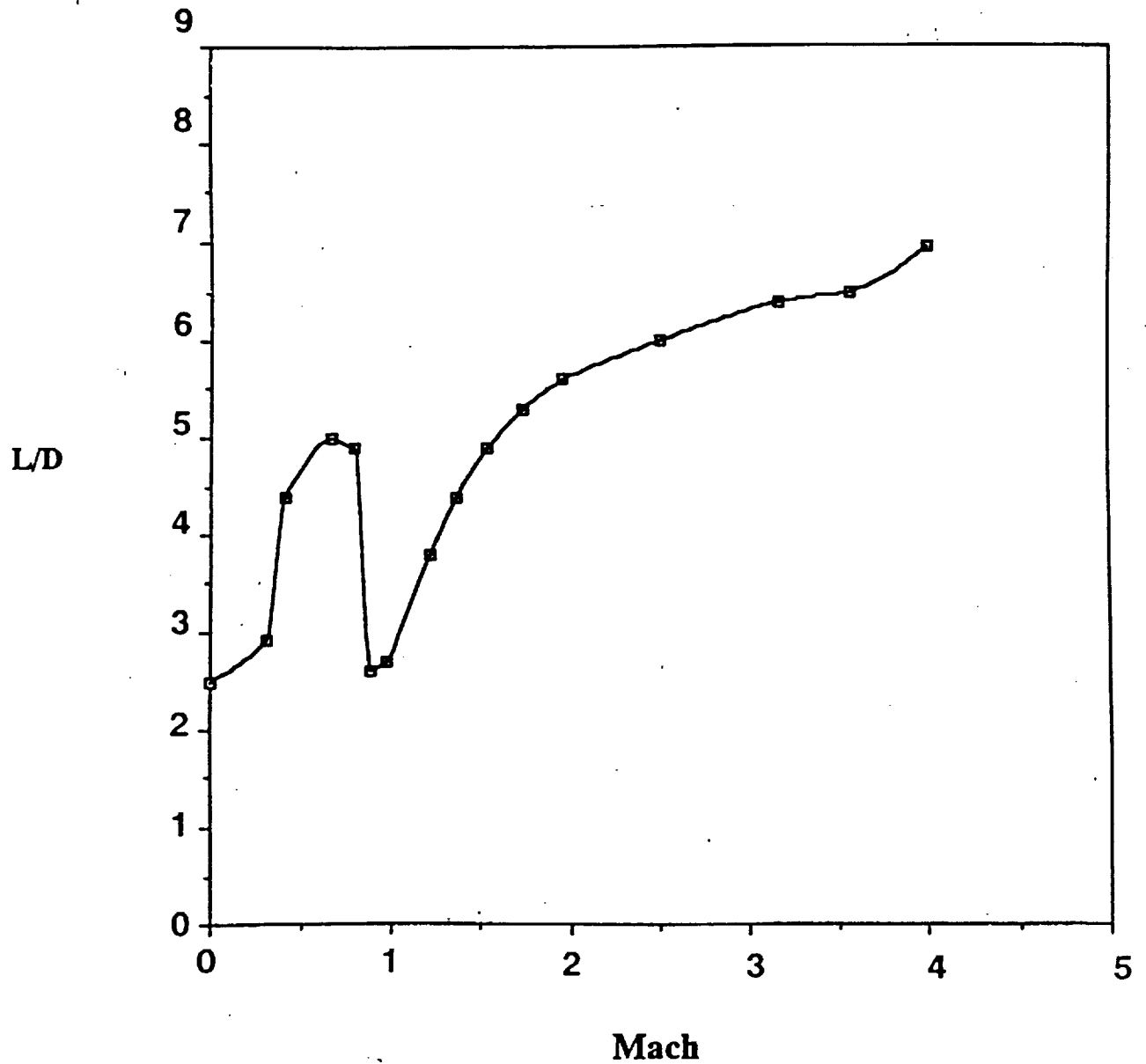


Figure 13. L/D versus Mach number flight regime

high lift coefficients but increases in the subsonic region as speed increases and angle of attack lowers. In the transonic region, the drag increases and the lift to drag ratio decreases.

## SUPERSONIC / HYPERSONIC AERODYNAMICS

The waverider is an extremely efficient vehicle in the supersonic flight regime. Whereas most conventional aircraft are lower in lift to drag due to wave drag, the waverider is designed essentially to ride on the shock much like a surfboard riding on top of a wave. The upper surface would be exposed to free stream conditions while the lower surface would be subjected to high pressure due to the pressure increase behind the shock.

Since most of the mission requires flying at cruise conditions, the design required a high aerodynamic efficiency in order to lower the drag and increase range. A cruise speed of Mach 4 at 80,000 feet was chosen to eliminate the need for an extensive cooling system and also reduce the demand on the engines. A program was written to calculate the drag based on skin friction and wave drag. References 5 and 6 were used for these drag estimates also linear theory was used. A graph of the drag component build-up can be seen in figure 14.

As the Mach number increases to its design point, the lift-to-drag ratio increases. MAXWARP calculated a L/D of 8.26 for the base waverider, but a 20% increase in drag was

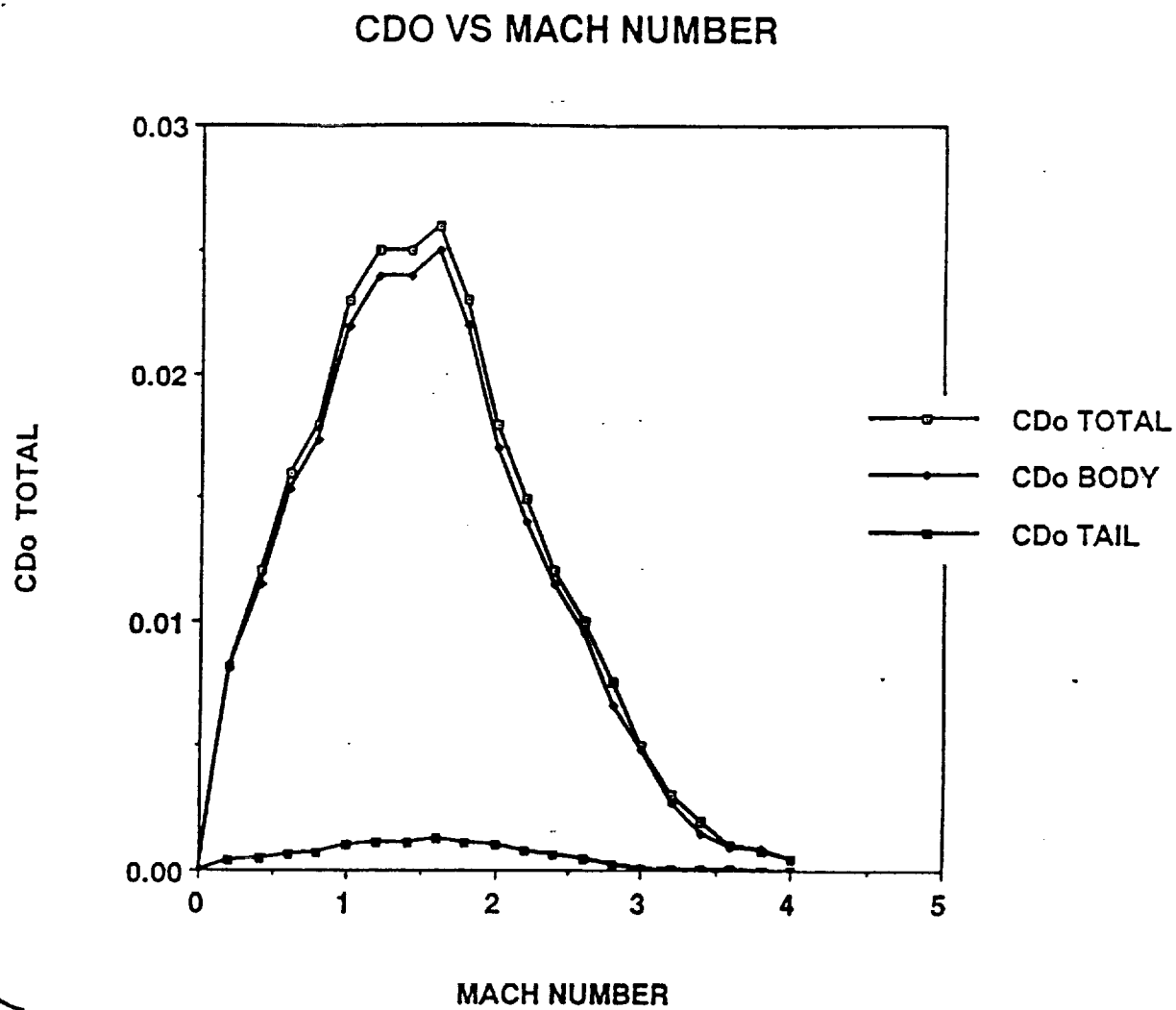


Figure 14. Drag component build-up

assumed due the addition of the tails and the engine box. Thus, the finalized L/D was 6.93 for the entire waverider.

## CHANGES TO BASIC WAVERIDER DESIGN

### BOATTAIL

Because of the large base area produced by the waverider design, the addition of a boattail was needed to reduce the pressure drag. The major center of the boat tail was integrated so that it helped in the expansion of the engine nozzles. The rest of the boattail was tapered down so that control surfaces could be placed on the vehicle. Due to the fact that the flow over the boattail was a three dimensional flow, an accurate drag calculation could not be attained. Therefore, an assumption was made on the percentage increase in drag due to the boattail.

### VERTICAL FINS

Twin tails were assumed to provide the stability of the aircraft. These tails were inclined to be parallel to the free stream and also to reduce the radar cross-section for stealth characteristics. A very thin supersonic airfoil would be needed to reduce drag at supersonic speeds.

### ENGINE BOX

The engine box was the most difficult addition to consider. Dimensions were obtained from the propulsion team and integrated into the program for drag calculations. The

engine box was designed to make the most efficient use of the flow field parameters. Since the number of engines is small, the box size would be small as well. This would reduce the wave drag.

## MISSION PROFILE

### INTRODUCTION

The main objective of the trajectory team was to determine the best possible flight path and performance of the hypersonic unmanned reconnaissance vehicle for a given mission. The mission requirements consisted of a naval vessel launch, flying to a cruise altitude of 80,000 feet or greater between the Mach numbers of 4 to 7, and cruising for a range of 6,000 nautical miles. The decision was made to launch conventionally from an aircraft carrier by means of a catapult launch, a climb to 80,000 feet, a cruise-climb at Mach 4 for a range of 6,000 nautical miles, followed by a minimum power descent to sea level. The advantage of higher Mach numbers was researched, and although they provide faster mission times, the materials and thermal protection systems needed to fly at these high speeds are heavy and costly. Therefore, the cruise speed was kept to a minimum.

### TRAJECTORY APPROACH

The trajectory analysis consisted of an integration of the aerodynamics and propulsion information. The main information requested of the aerodynamic team consisted of the coefficient of lift required for steady level flight at each Mach number and altitude, the drag polars at each altitude and Mach number, and the thrust required at steady-level flight which is equal to the drag. From the propulsion team, the thrust versus Mach number at various altitudes was required. Each of these two areas would be integrated to



determine the excess specific power needed to maneuver, accelerate, or climb. An attempt was made to write an algorithm to determine the specific power curves for the particular mission. Much time was spent trying to produce viable data and although some information was gained from the actual program, it could not be decided if the information was accurate since there was some contradiction. Due to limited time constraints, a program was written that would generate a constant dynamic pressure trajectory which was much simpler than the specific power curves. According to reference 7, a constant dynamic pressure trajectory approximated the minimum time-to-climb trajectory which was also similar to the minimum fuel-to-climb trajectory. Typical current-technology-high-thrust fighters stay low and accelerate to transonic speeds, then pitch up into a steep climb at approximately constant dynamic pressure to the optimal cruise speed and altitude. It was desired that the aircraft fly along a minimum fuel-to-climb trajectory to conserve fuel for the cruise portion of the mission. A constant dynamic pressure of 650 psf. was chosen which is the dynamic pressure at cruise conditions.

#### **TAKE-OFF AND CLIMB CHARACTERISTICS**

A naval launch presented several difficulties namely the limited takeoff distance. Several different ideas were circulated amongst the team members concerning take-off possibilities. The length of an aircraft carrier deck is approximately 1,000 feet which is too short for most

conventional aircraft to accelerate to take-off speed. The thrust-to-weight ratio required for this approach would be much greater than one, not to mention the difficulty of clearing the deck and safety considerations. A rocket-assist was considered as a possible solution; however, this required a heavier aircraft and the dangers involved to the crew members negated this type of approach. The conventional catapult launch was decided upon as the safest and most economical approach to take-off. Most naval catapult launches are limited to the weight of the aircraft. The most powerful catapult system currently in use by the Navy is limited to aircraft weighing 100,000 pounds or less. This catapult system is capable of accelerating a 100,000 lb. aircraft to speeds of 120 knots. This was the major factor in limiting the aircraft to the maximum 100,000 lb. weight limit. The take-off wing loading was 43.5 pounds per square foot. The take-off velocity consisted of 110 knots contributed by the catapult system and 20 knots wind-over-deck resulting in a velocity of 130 knots. Since delta wing aircraft with a low aspect ratio generally have a low maximum lift coefficient, a flap system was needed for launch. It was determined using reference 7 and 8 that with plain flaps deflected  $10^\circ$  upon take-off, a  $\Delta C_l = 0.35$  could be achieved resulting in a maximum lift coefficient at take-off of approximately 1.4. This determined the stall speed of 97.3 knots. Actual lift coefficient at take-off was 0.79 with an angle of rotation of  $14^\circ$  after the aircraft leaves the deck.

The climb from sea level to the cruise altitude of

# ALTITUDE vs. MACH NUMBER

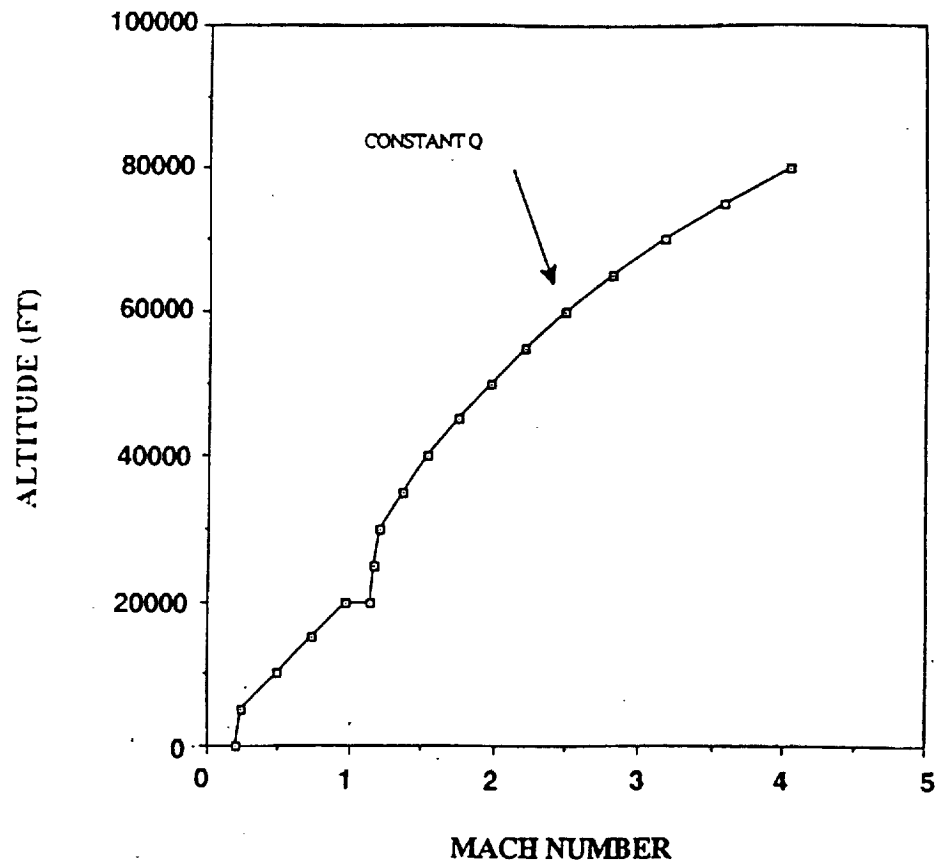


Figure 15. Dynamic pressure trajectory

# RATE OF CLIMB VS. MACH

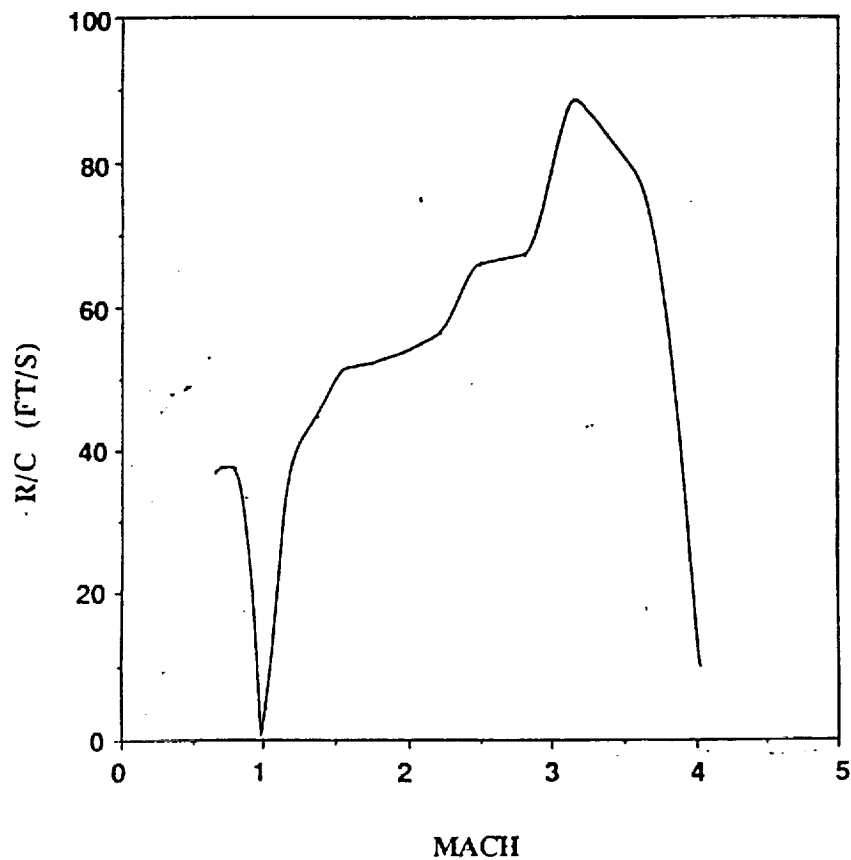


Figure 16. Rate of climb versus Mach number

# WEIGHT vs. TIME

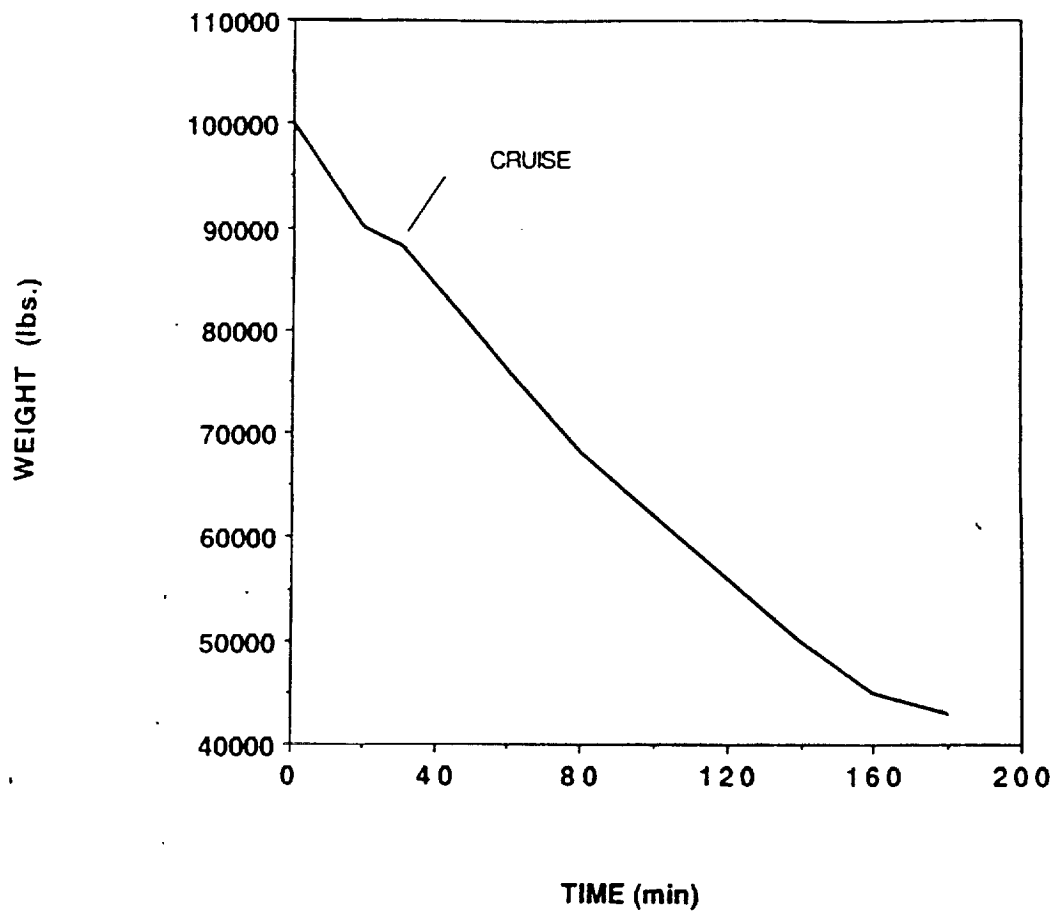


Figure 17. Weight versus time

# ALTITUDE vs RANGE

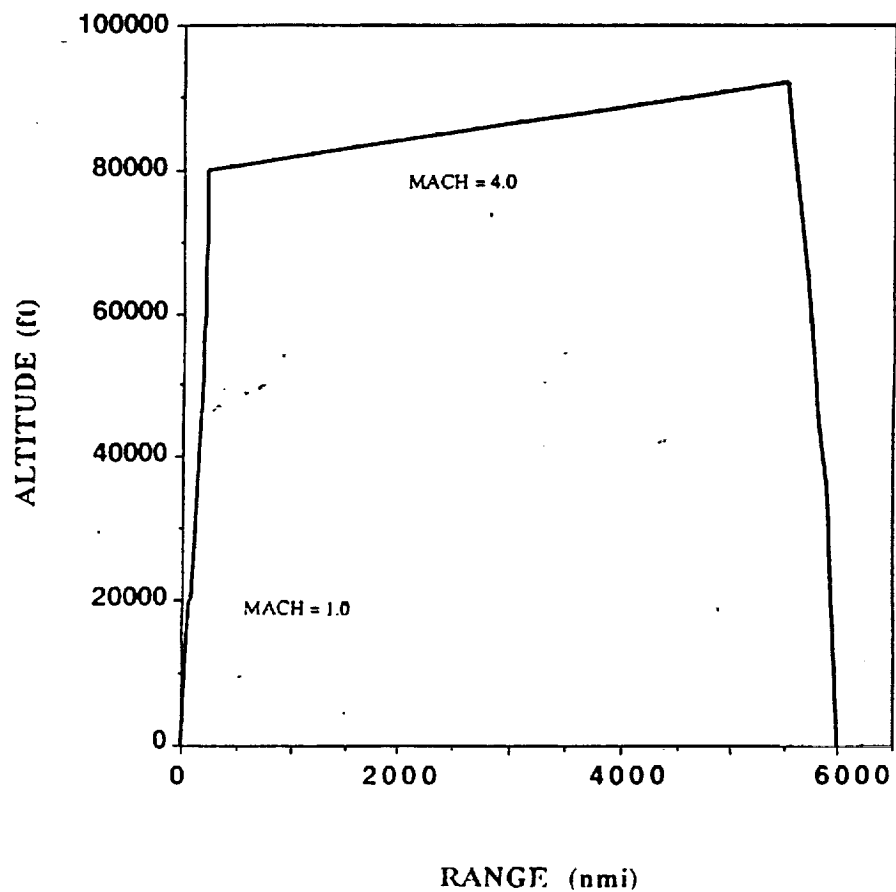


Figure 18. Altitude versus range

80,000 feet will be accomplished while keeping a constant dynamic pressure of approximately 650 pounds per square foot. See figure 15. This consisted of a linear transition to a Mach number of 0.66 at a constant rate of climb of approximately 38 feet per second. The aircraft would level off in the transonic region with as little as  $1/10 g$  acceleration to get through the thrust pinch and then assume a constant dynamic pressure trajectory to cruise altitude. The rate of climb versus Mach is shown in figure 16. The aircraft burns approximately 12,000 pounds. of fuel to reach cruise conditions as can be seen in figure 17.

#### CRUISE

A general diagram displaying the altitude versus range for the aircraft is shown in figure 18. It can be easily seen from figure 18 that only about 250 nautical miles was covered by the time the cruise altitude was reached. The decrease in weight due to fuel usage caused a typical cruise climb to occur. To maintain the best aerodynamic efficiency during cruise, as fuel was burnt, the dynamic pressure was lowered resulting in a climb to a final height of 92,500 feet from an initial 80,000 feet at the start of cruise.

Figure 19 displays the lift-to-drag ratio versus Mach number which shows an increase in lift-to-drag in the subsonic region, decreasing in the transonic region and then increasing to the waverider's design point of 6.93 due to the efficiency of the waverider at high Mach numbers. Maxwarp predicted a baseline  $L/D=8.26$  but due to base drag and drag from other components, the maximum lift-to-drag decreased.

## DESCENT AND LANDING

A minimum-powered descent was chosen for the trajectory to minimize the fuel consumed. The angle of descent was approximately  $8.21^\circ$  covering a distance of 105.5 nautical miles. The aircraft would return for a carrier arrested landing. This may pose some problems if the aircraft missed the arresting hook on the first try, it may be difficult to push full throttle and go around for another try since the aircraft is unmanned. There may also be a safety risk involved for an unmanned vehicle landing on the carrier.

The wing loading upon approach is approximately 18.7 pounds per square foot. With flaps deflected  $15^\circ$ , a maximum lift coefficient of 1.57 can be achieved resulting in a stall velocity of 66.3 knots. An actual landing velocity of 76.2 knots with an angle of attack of  $20^\circ$  was used to maintain speeds above stall.

## MAP PROFILE

The simple geographical map shown in figure 20 displays a typical mission for this particular aircraft. The aircraft would take-off from a carrier group in the Indian Ocean and fly 6,000 nautical miles covering a great portion of the Middle East countries and return hopefully undetected to the same carrier group. The mission involves a 2-g turn halfway during the course to limit structural stress at high speeds. Three different missions were proposed: a carrier-to-land mission, a carrier-to-carrier mission, and a carrier-and-return mission. The latter was chosen since it provided the

least amount of complication in logistics, communication, and stealth.

## L/D v. Mach for Mission

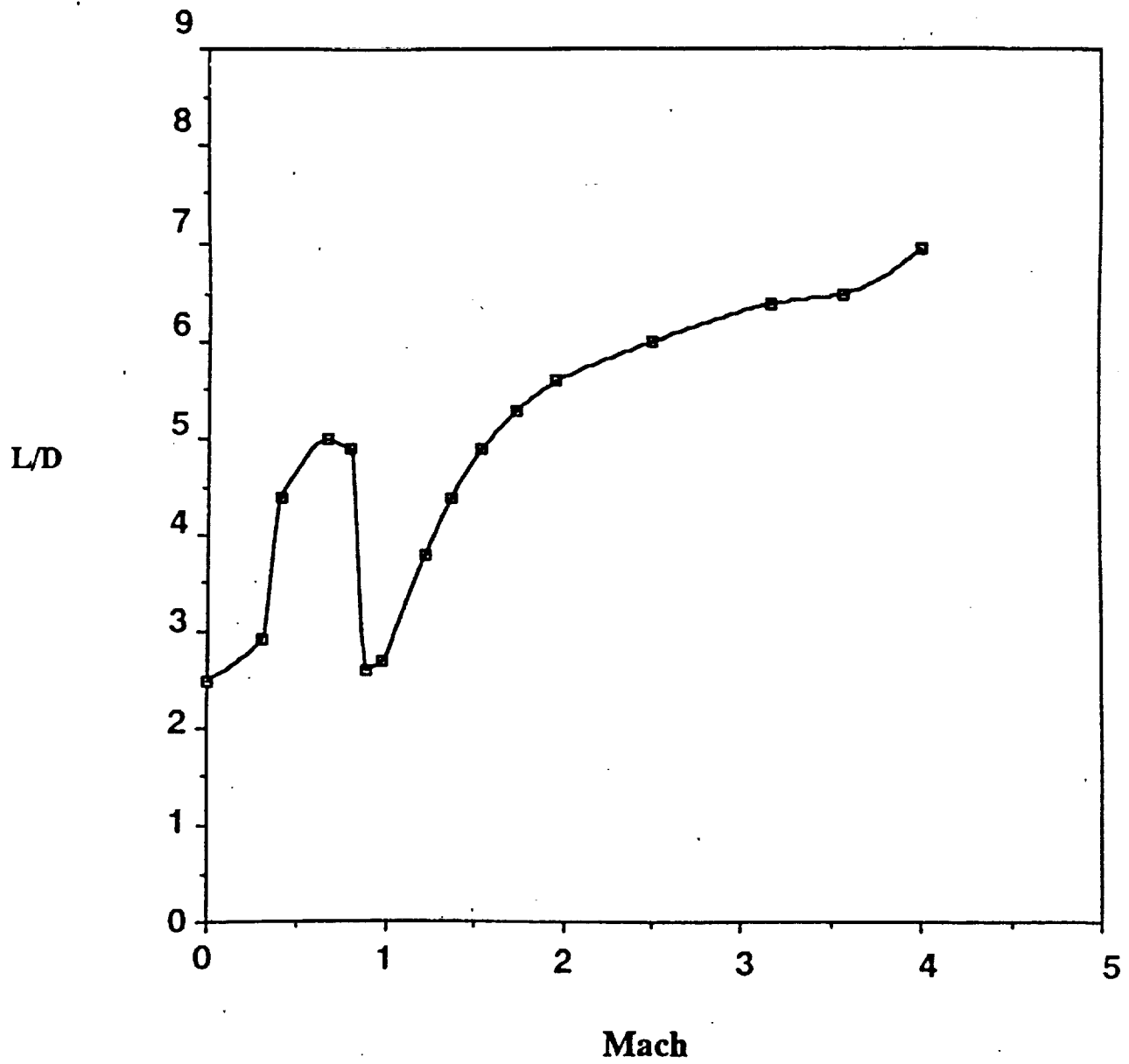


Figure 19. L/D versus Mach number for mission profile



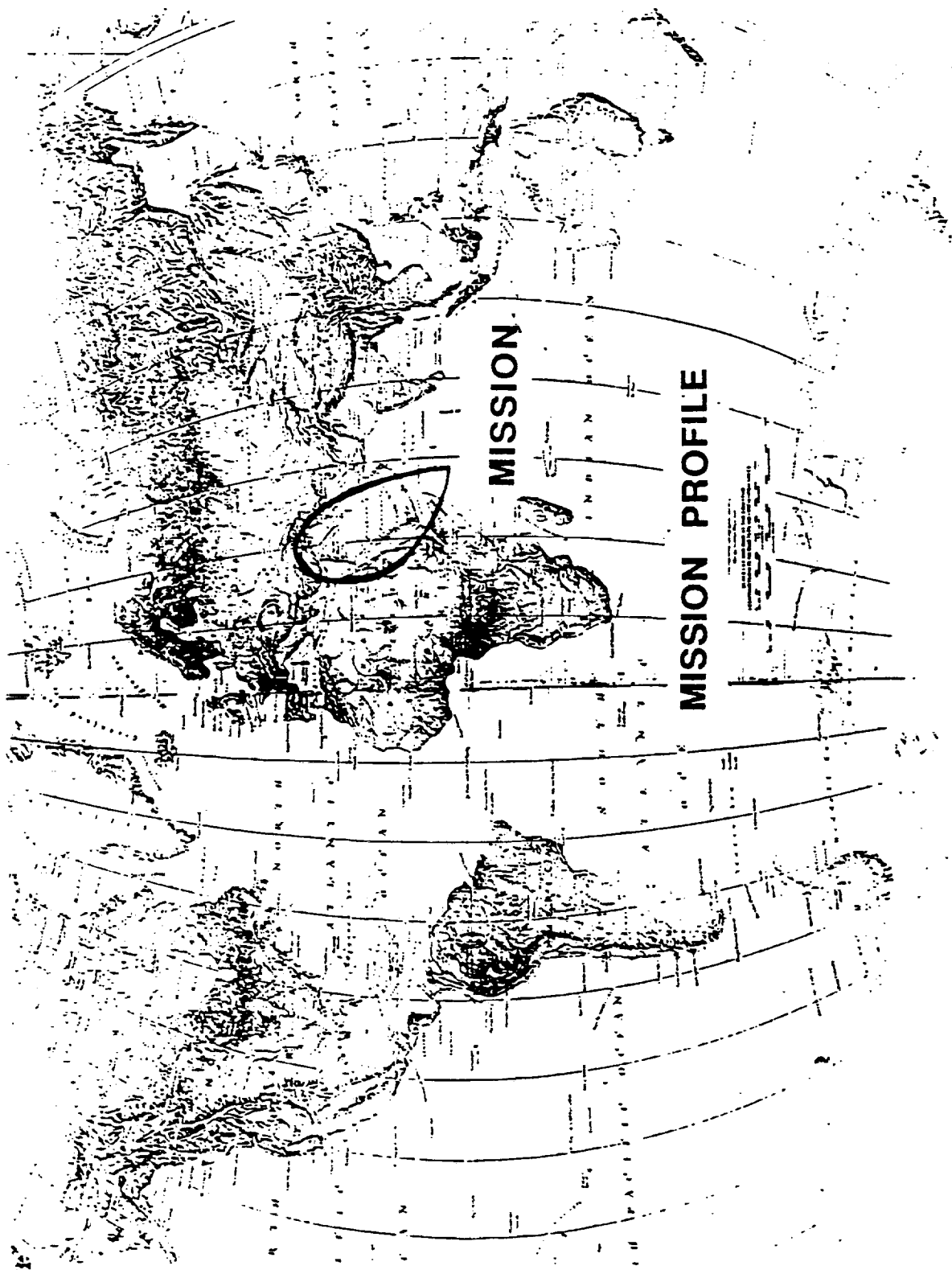


Figure 20. Geographical mission profile

## PROPULSION SYSTEM

In the design of any aircraft, the selection of the propulsion system is crucial to the aircraft's size and performance. The engine type and performance influences the cruise range, speed, and altitude. In the case of a hypersonic vehicle, the influence is magnified.

The mission specifications for this project all play an important role in the selection of the propulsion system. The most influential of these requires the vehicle to be launched from an aircraft carrier. This requirement creates some unique and challenging propulsion problems: short take off distance, limited aircraft size and volume, and storage/handling of fuel.

The first implication of a carrier launch is rather straight forward. The propulsion system and catapult must accelerate the aircraft to take off speed in less than 350 feet. This requires that the aircraft generate a large amount of static thrust.

Fuel volume and total aircraft weight are very much limited for a carrier based aircraft. In order to fit onto the carrier elevator, an aircraft must be smaller than 80x70 feet. The poor volume efficiency of the waverider, chosen for its aerodynamic performance, puts a fuel volume limit of 3000 cubic feet on the design. In addition to these restraints, the total aircraft can weigh no more than 100,000 pounds in order to qualify for catapult launch.

The storage and handling of fuel in the closed

environment of the aircraft carrier is also a primary concern. Any potential performance benefits of a hazardous fuel must be considered against the needed storage facilities and dangers posed by the use of the fuel.

With each of these unique problems in mind, various fuels and engine systems were examined. As an initial investigation into possible fuel choices, the fuel volume required to cruise 6000 nautical miles was plotted for liquid hydrogen, liquid methane, and JP-X. Figure 21 shows the differences in these volumes. With an available fuel volume of 3000 cubic feet, liquid hydrogen was much too voluminous. Liquid methane was considered, but the performance improvements over JP-X were not considered large enough to outweigh the potential risks and complications it would cause aboard an aircraft carrier. JP-X easily meets the volume restrictions, and is greatly favored by the Navy over any cryogenic fuel. Thus, JP-X was chosen to fuel the propulsion system.

The use of JP-X as fuel limits the cruise speed to Mach 4. This is due to the thermal breakdown of JP-X at temperatures encountered above Mach 4.

The choice of Mach 4 as a cruise speed and JP-X as a fuel enabled various engine types to be considered. The air-turbo rocket (ATR), turbofan, turbofan/ramjet, and ramjet all provide good performance and thrust during the cruise portion of the mission. Figure 22 shows a comparison of specific fuel consumption vs. specific thrust of each engine at cruise

### Fuel Volume vs Range for M=4

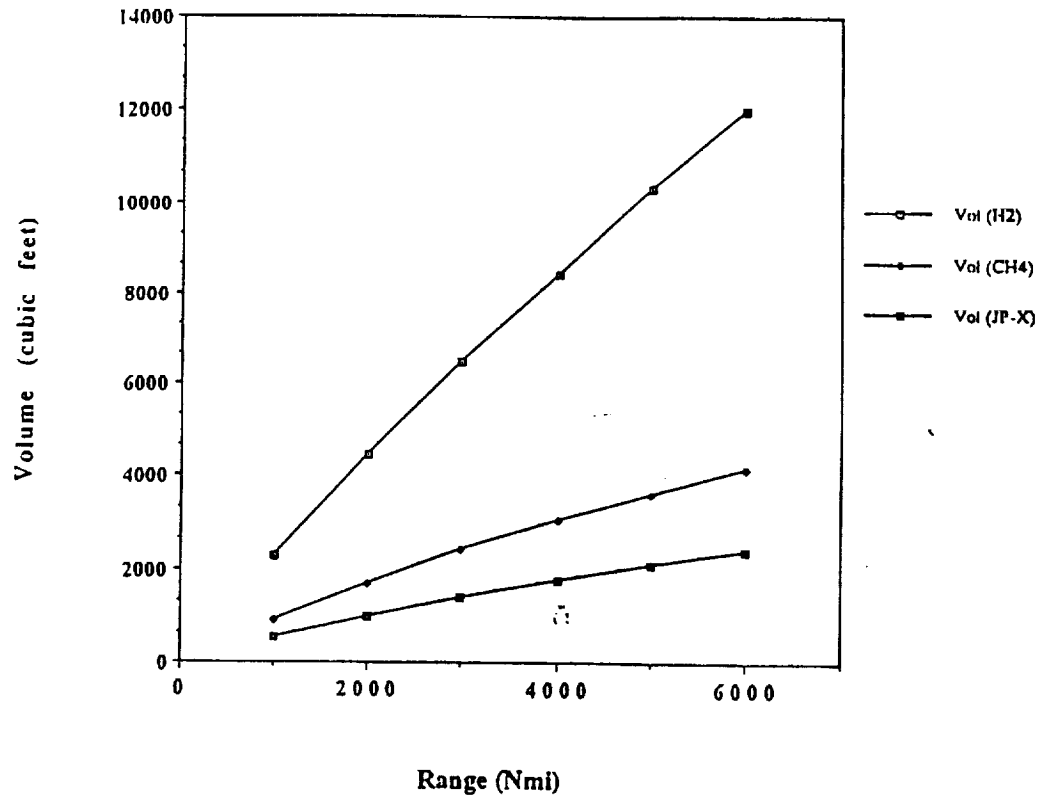


Figure 21. Fuel volume versus range

### Specific Thrust vs SFC

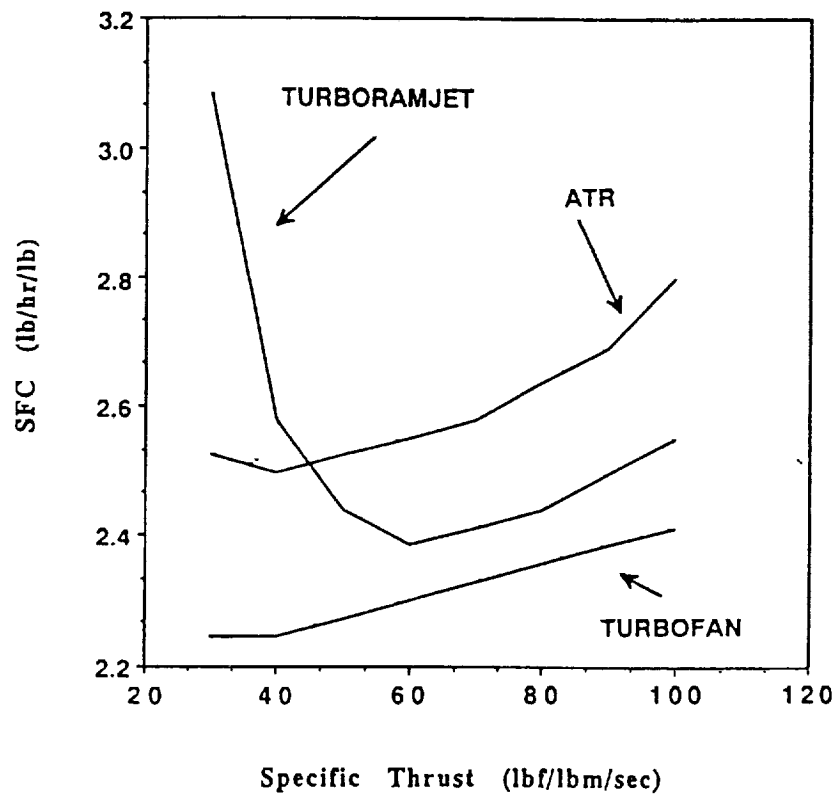


Figure 22. SFC versus specific thrust

conditions (Mach 4 at 80,000). This graph shows the best fuel consumption is provided by the turbofan. With this advantage in fuel performance, the turbofan was selected to power the aircraft.

The engine and fuel selected, sizing of the engine was considered. The thrust required to climb to the cruise altitude was calculated in the mission profile program. By comparing the required thrust to climb to the available thrust from the General Electric engine data (reference 10 ), it was seen that the engine needed to be 10% larger than the provided size in order to meet the required cruise thrust in the most efficient manner.

In order to convert the engine data from methane to JP-X fueled, fuel flow was multiplied by the heat of combustion of liquid methane and divided by that of JP-x. When the engine data was converted and scaled, it was plotted against the required thrust to climb in figure 23. From this figure it was seen that the engines provided sufficient thrust across the entire mission profile. Thus, the engines were scaled to cruise using a scale factor of 1.1.

The resulting specific fuel consumption against Mach number is seen in figure 24. Thrust available is compared to drag in figure .

In summary, The trade study described above showed that two JP-X fueled turbofans provide the most efficient operation across the entire mission profile for this design.

The final engine dimensions are shown in figure 25.

# THRUST vs MACH NUMBER

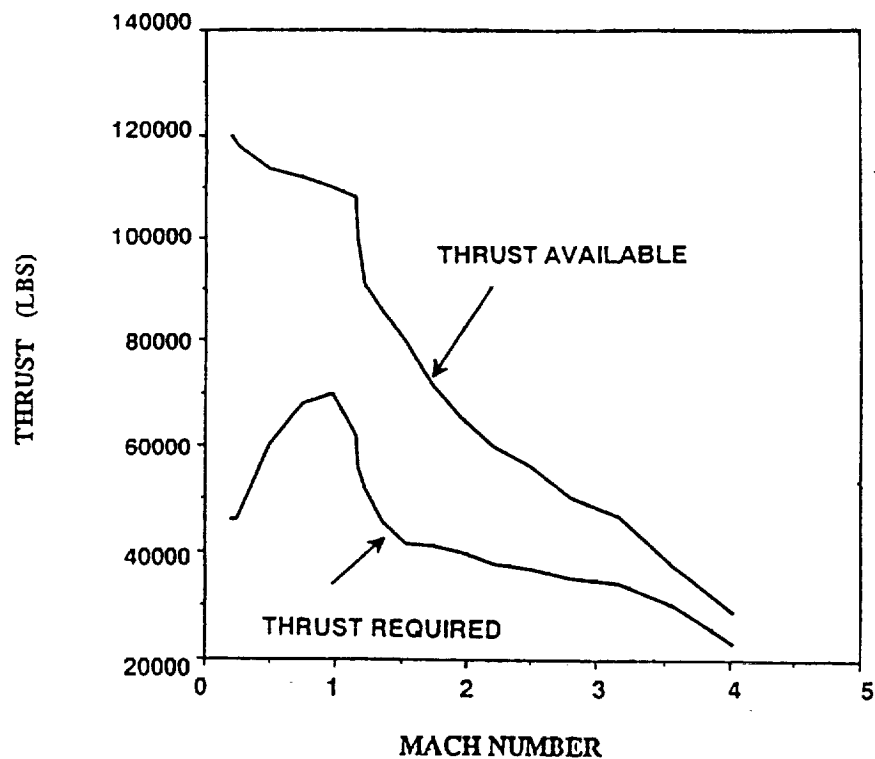


Figure 23. Thrust versus Mach number

# SFC vs MACH NUMBER (JP-X FUEL)

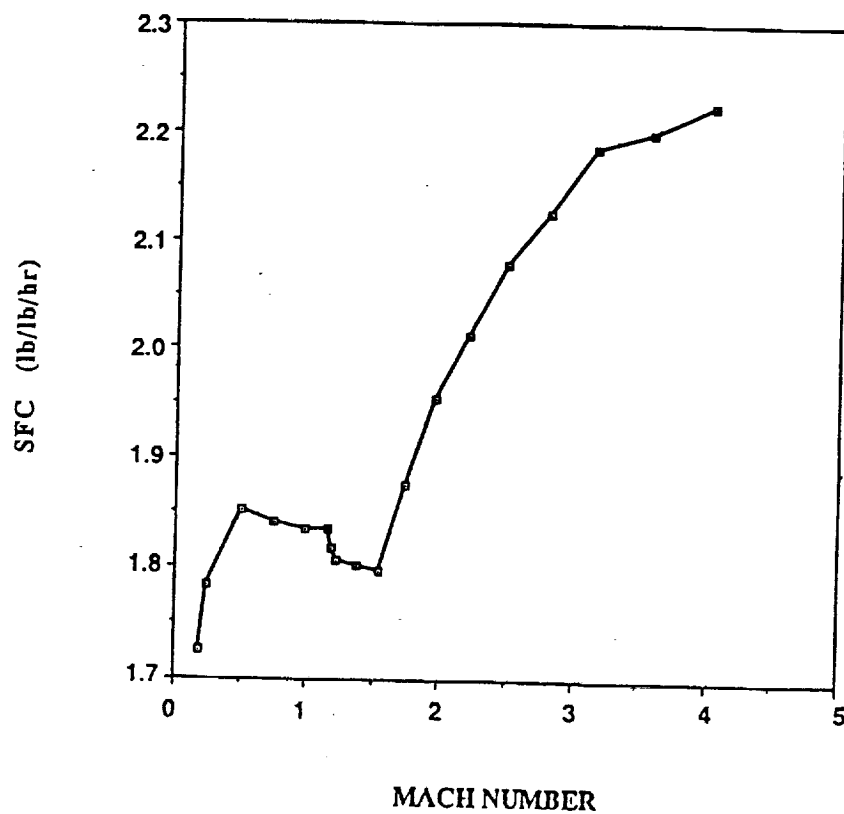
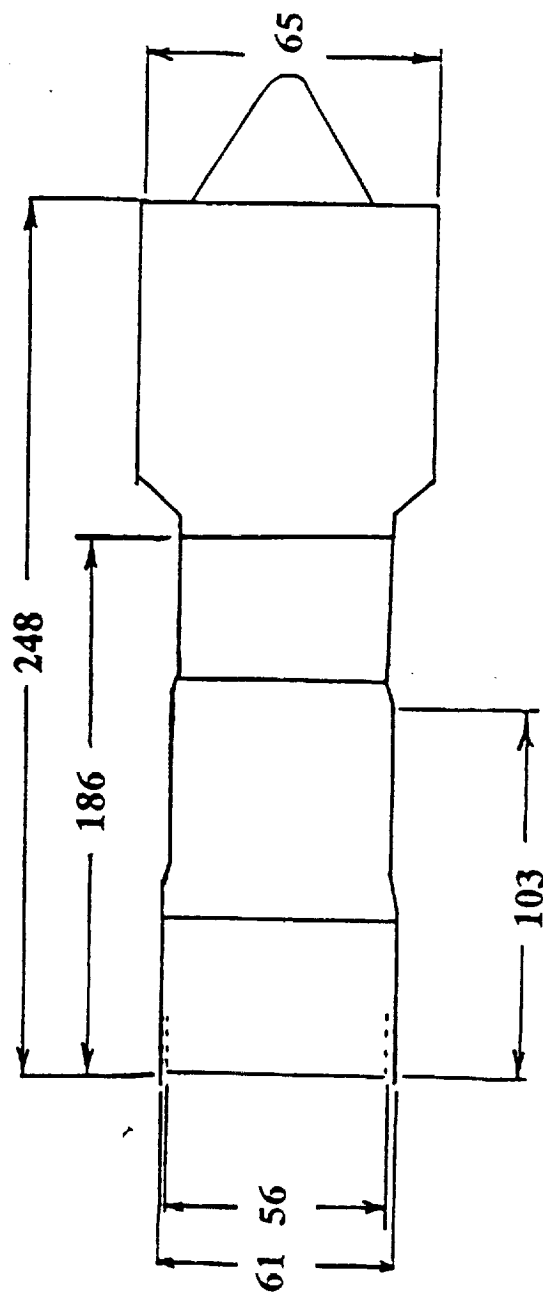


Figure 24. Fuel consumption per Mach number

# ENGINE DIMENSIONS (inches)



**Engine Weight: 2 x 7000 lb**

Figure 25. Final engine dimensions



## ENGINE INLETS

One of the most important features on a hypersonic aircraft is its inlet. Inlet configuration is one of the aircraft's parameters that determines the maximum speed an aircraft can achieve. For most subsonic and supersonic jet-powered aircraft, round simple inlets are used. However, at high supersonic and hypersonic speed (above Mach 3.5) round simple inlet have a severe stagnation pressure loss. Thus, for this aircraft a mixed compression inlet is required. The design of the inlet was treated as one dimensional flow. Each shape and compression effect of the shock waves were computed using shock expansion theory. In trying to determine the number of ramps required and length of the inlets reference 3 was referred to. According to Nicolai, Mach 4 cruise speed requires at least 4 oblique shocks to meet military specification for stagnation pressure lost. Stagnation pressure lost at Mach 4 was no less than 0.6695 .

As a result, a preliminary design incorporated three compression ramps to slow down air flow entering the normal shock at the inlet throat. However, the best design could only yield a pressure lost of 0.581. The second and last design used four compression ramps, yielding seven oblique shocks and a total pressure lost, from the aircraft nose shock to the engine first compression face of only 0.857 (see figure 26). Using the geometries of each ramps, the four feet width of the inlet and the required 194.36 pound per

second air flow, including engine bleed flow, (reference 5) the inlet height is determined to be 3.127 feet. These four ramps, with the initial shock from the aircraft nose, were able to slow the flow down from Mach 4 to Mach 1.254. Immediately after the normal shock at the throat the flow slowed to Mach 0.81. Next a subsonic diffuser was required to slow air flow down to Mach 0.4 at the engine first compressor face.

Size of the entire inlet was determined from required capture area, ramps geometries and engine size. The length of the compressor portion of the inlet was 12.06 feet, and length of the diffuser was estimated at 10 feet. The Nicolai text was also used to estimate the boundary layer duct required to divert boundary layer flow from the inlet. This area was found to be 1.297 square feet, translating to roughly four inches high.

Required sizing of the inlet for subsonic was beyond the ability of the designer.

# INLET DESIGN

MIXED COMPRESSION  
· SEVEN VARIABLE RAMPS

PRESSURE RECOVERY  
·  $0.86 * P_o$

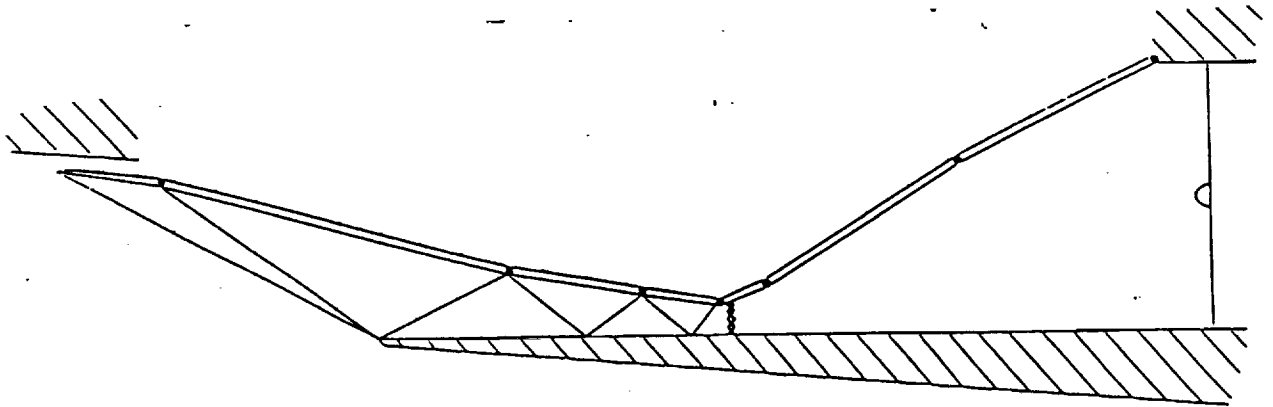


Figure 26. Inlet design

## WEIGHT ANALYSIS

The weight analysis for this vehicle was conducted with HASA, a weight and sizing program for hypersonic vehicles. Important inputs into the program include length, % fuel weight, engine type, and approximate dimensions of the aircraft.

The most important sizing input for this program is the % fuel weight. HASA<sup>4</sup> takes several equations of aircraft component weights and iterates until all equations are satisfied. A markedly different total weight resulted from various inputs of % fuel weight. The maximum allowed takeoff weight was known previously, so the % fuel weight was changed until the total weight was 100,000 lbs. The component weights were then given by the program for this configuration.

The weights are as follows:

fuel:	60,300 lbs
engines:	14000 lbs
metal structure:	8500 lbs
payload:	7500 lbs
avionics:	4200 lbs
landing gear:	3800 lbs
electronics:	950 lbs
thermal protection:	400 lbs
hydraulics:	350 lbs

These weights also give us the maximum % fuel weight of any total weight under 100,000 lbs. Thus this configuration,

although approximate, is the most efficient weight under the total weight constraints.

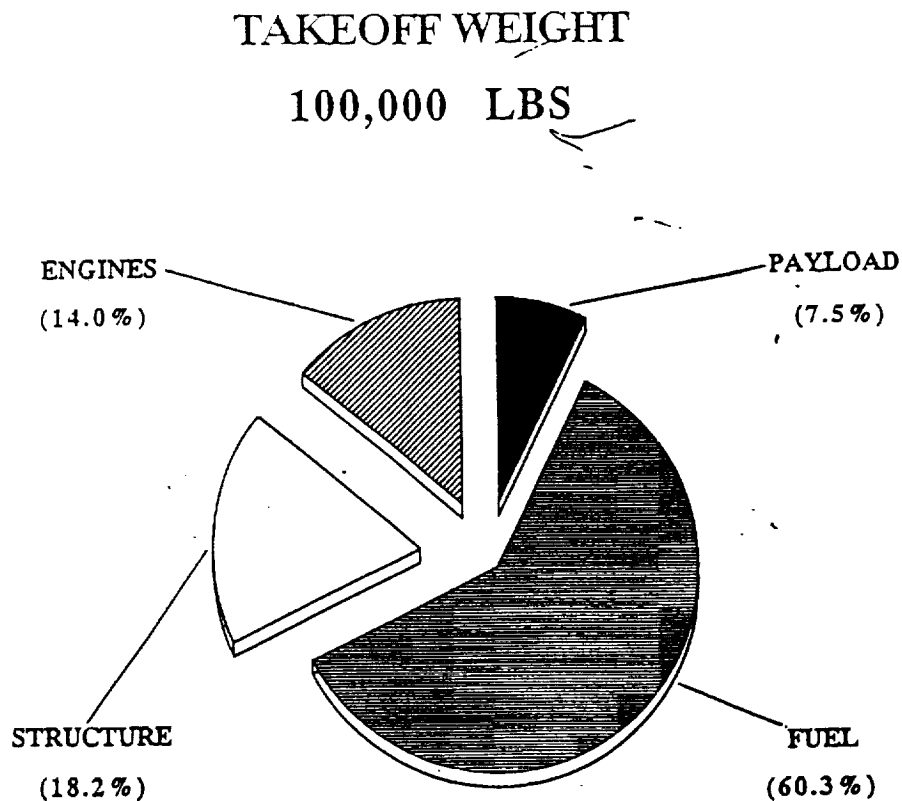


Figure 27. Take-off weight pie chart

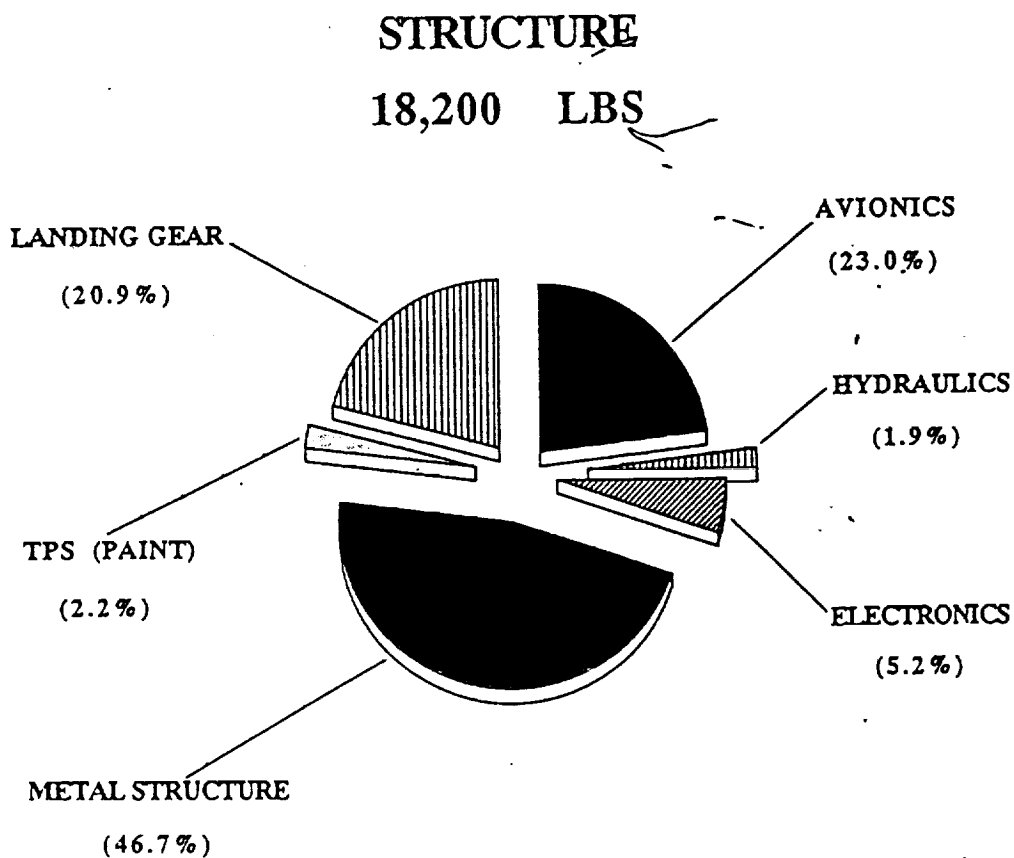


Figure 28. Structural pie chart

## INBOARD PLANFORM

The inboard planform was important to show how efficiently the volume of this waverider could be used, and to keep the static margin small enough to be controllable with most control surfaces.

Most of the volume available in a waverider is in the rear of the plane due to its slim shape. A structural boundary around the outer surface of the plane was assumed to be 9 inches on the bottom and 3 inches on top for simplicity. Thus, the parts of the plane where there was less than 1 foot of thickness of the plane could not be used for storage.

The nose gear was the most difficult object to position. The nose gear was placed 15 feet from the nose of the 70 foot aircraft. With the 10-foot length, the front tires rest tightly in the body center 25 ft from the nose. The avionics and payload had small volumes and were placed just behind the landing gear, using all of the usable volume behind the nose gear in order to leave necessary volume for fuel tanks.

The four fuel tanks have a total volume of 1200 cubic ft. More than half of the fuel is placed in a conformal volume between the payload and the main landing gear. The main landing gear are 59 feet from the nose, folding toward the center of the aircraft. A space of 12 feet is maintained between the gear to include partial inclusion of the engines into the body for compactness. The remaining fuel tanks are placed above and to the sides of the engines to minimize fuel pumping distances.

Less than half of the total volume of 5250 cubic feet is

used. However, every component of the aircraft is totally contained within except for most of the engine box. Also, the largest static margin is less than 9 percent of the aircraft length, which is controllable.



**VOLUME  
5250 CUBIC FT**

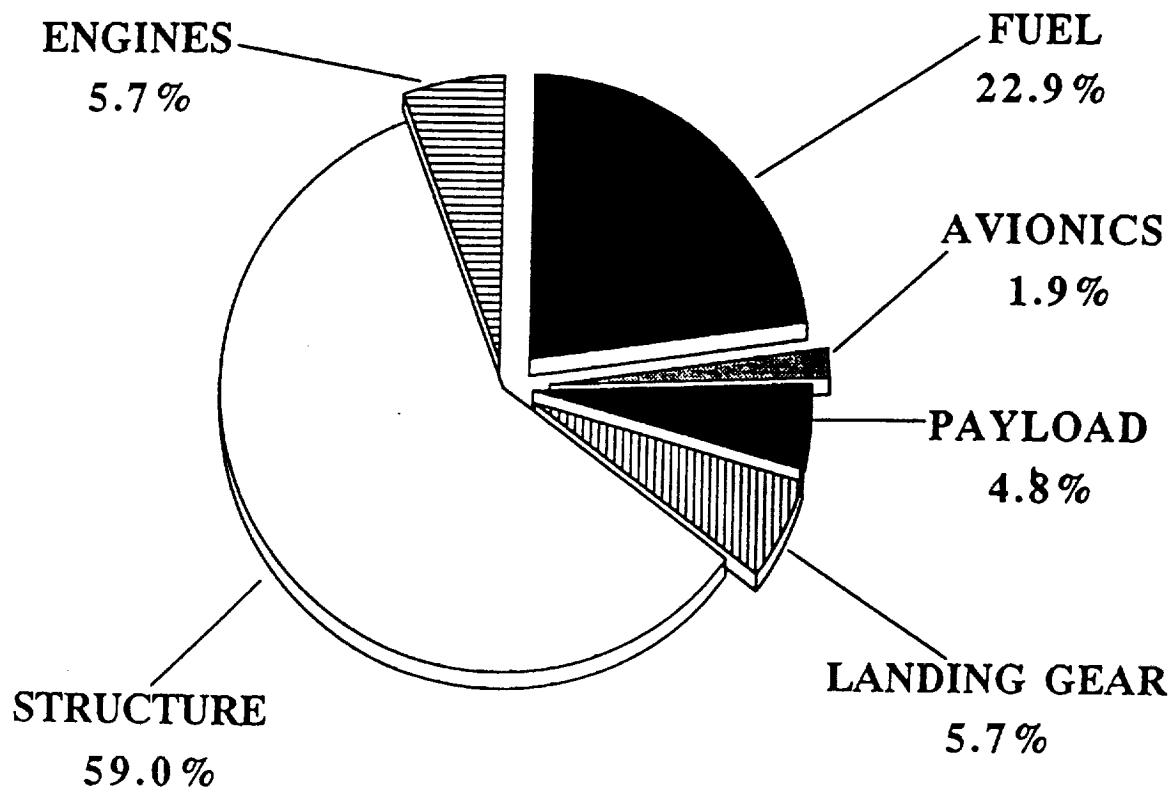


Figure 29. Volume pie chart

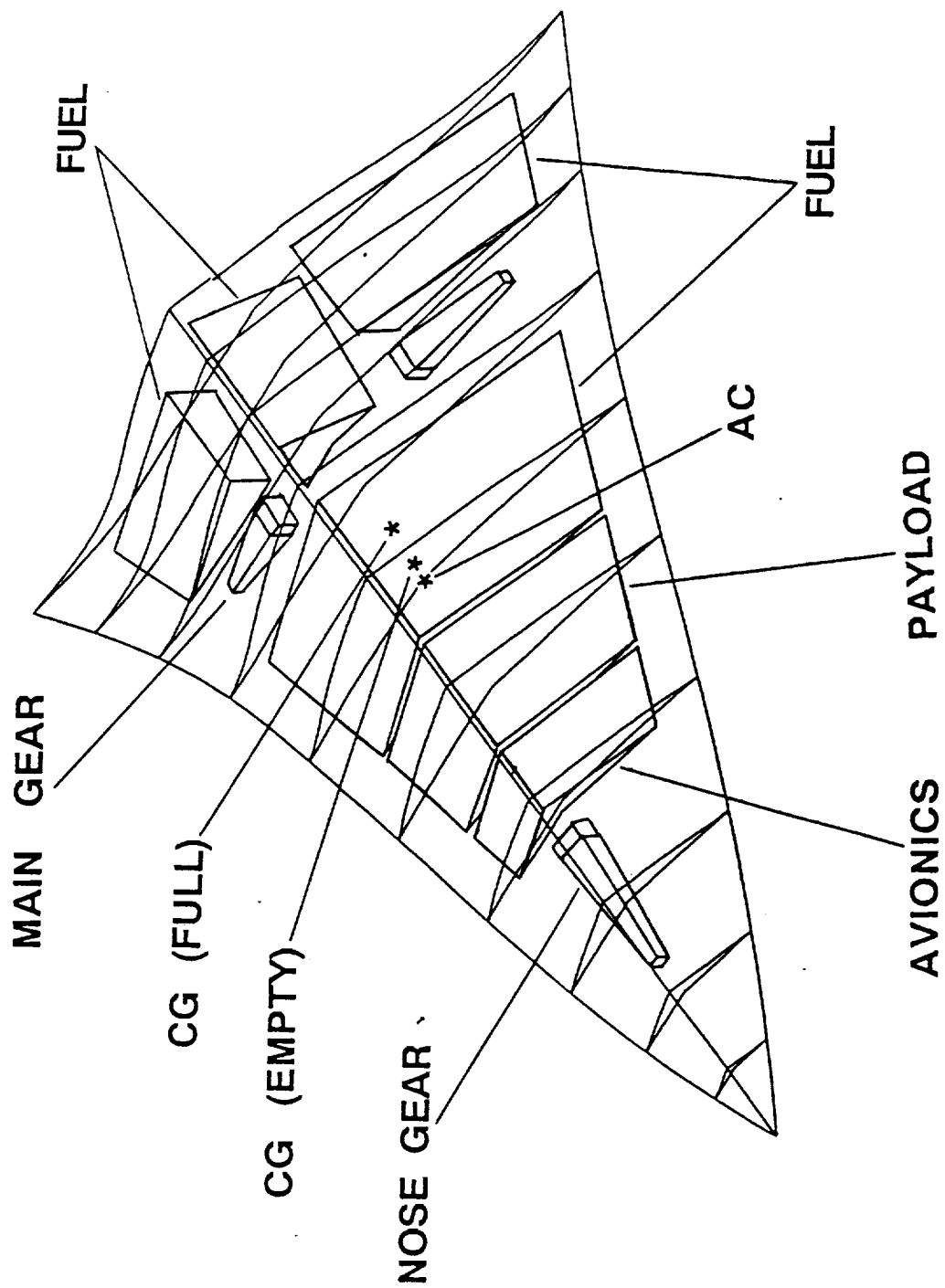


Figure 30. Planform view

## THERMAL PROTECTION SYSTEMS

The design of a thermal protection system (TPS) depends on the temperatures and heat flux encountered. Physical geometry and trajectory are the driving factors of our TPS design. When this vehicle is flying at hypersonic speed it will encounter a vast region of very high temperatures at the nose and along the leading edges. Therefore the application of different alloys at various areas of the aircraft is required to keep control of the temperature and reduce material breakdown.

Appropriate materials that could withstand these temperatures were evaluated. For our purposes the alloy Ti-8AL-1 Mo is best suited for the hottest spots of the aircraft which would include the nose, inlets, and along the leading edges. The high temperature alloy A-L 18NiCoMo met temperature requirements at all other cooler spots on the aircraft skin. When deciding on a material, good high temperature characteristics and high emissivities are of the utmost importance. All specifications of the two materials are listed in material selection list.

The aircraft has a passive cooling system by the use of several coats of "iron ball" black paint applied to the entire surface area to assist in the irradiation of heat from the aircraft skin. Figure 31 illustrates a comparison of cross-sectional views for three different passive systems. The second system, which is a titanium matrix composite, will be our application. The first and third systems are used for

## MATERIAL SELECTION FOR THE LEADING EDGES AND AT THE NOSE.

### Ti-8Al-1Mo

Physical constants:

Specific gravity	4.37
Density, lb./cu. in.	0.156
Thermal coef expansion/ degree FE-6	
68-212 degrees Fah.	4.7
68-572 degrees Fah.	5.2
68-1200 degrees Fah.	6.0
Electrical resistivity, microhm-cm	
at 75 degrees Fah.	198.6
at 1200 degrees Fah	203.4
Thermal conductivity, cal/cm**2/cm/sec/degree celsius	
at 75 degrees Fah.	0.0143
at 1200 degrees Fah.	0.0299
Modulus of elasticity, psi E6	
at 75 degrees Fah.	19.12
at 716 degrees Fah.	16.45

## MATERIAL SELECTION FOR FORWARD, MID, AND AFT FUSELAGE AREAS

### A-L 18NiCoMo (250)

Physical constants:

Density, lb./ cu. in.	0.289
Modulus of elasticity, psi E6	26.5-27.5
Modulus of rigidity, psi E6	10.2
Thermal coef. expansion/ degree Fah. E-6	
70-900 degrees Fah.	5.6
Electrical resistivity, microhm-cm	
annealed	60.5
aged	38.5

higher temperature purposes and would be much more expensive. The major advantage of passive thermal protection is weight. Not needing an active cooling system will make our aircraft that much lighter.

Temperature distribution varied as a function of mach number exponentially. All numbers produced were from an in-house program derived from algebraic equations in CDHEAT. A radius of one inch was used to affirm the use of a sharp leading edge. Gamma value of 1.4 was used because the temperatures dealt with were not hot enough to dissociate the diatomic molecules into monatomic molecules. For most stealth aircraft emissivity is in the range of 0.8 to 0.9. An emissivity of 0.85 was chosen purely as a mean value.

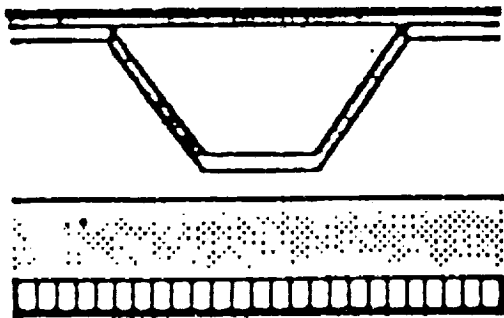
Stagnation temperature is more or less a given as it is a function of free stream velocity and temperature. However, the temperatures at the nose and along the leading edges are a little more involved. The theory involved included setting convection equal to radiation to achieve necessary adiabatic conditions.

The conformal temperature map (CTM) gives a visual representation of the magnitude of temperatures on the top and bottom surfaces. The results produced were once again from an in-house program derived from relations in CDHEAT. A radius of 1/8 of an inch and an emissivity of 0.83 was used for this analysis. Gamma stayed the same as described above. Other major concerns to be pointed out from the CTM is how much hotter the bottom surface is, and how temperature changes along the leading edges as sweep angle constantly

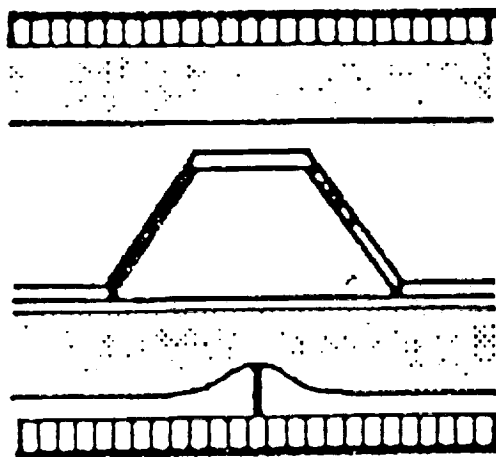
# Passive Thermal Protection



- Carbon/Carbon
- Q Felt



- Ti Matrix Composite
- Q Felt
- Graphite/Carbon



- Graphite/Epoxy
- Q Felt
- Ti Matrix Composite
- Fiber Max
- Carbon/Carbon

Figure 31. Passive thermal materials

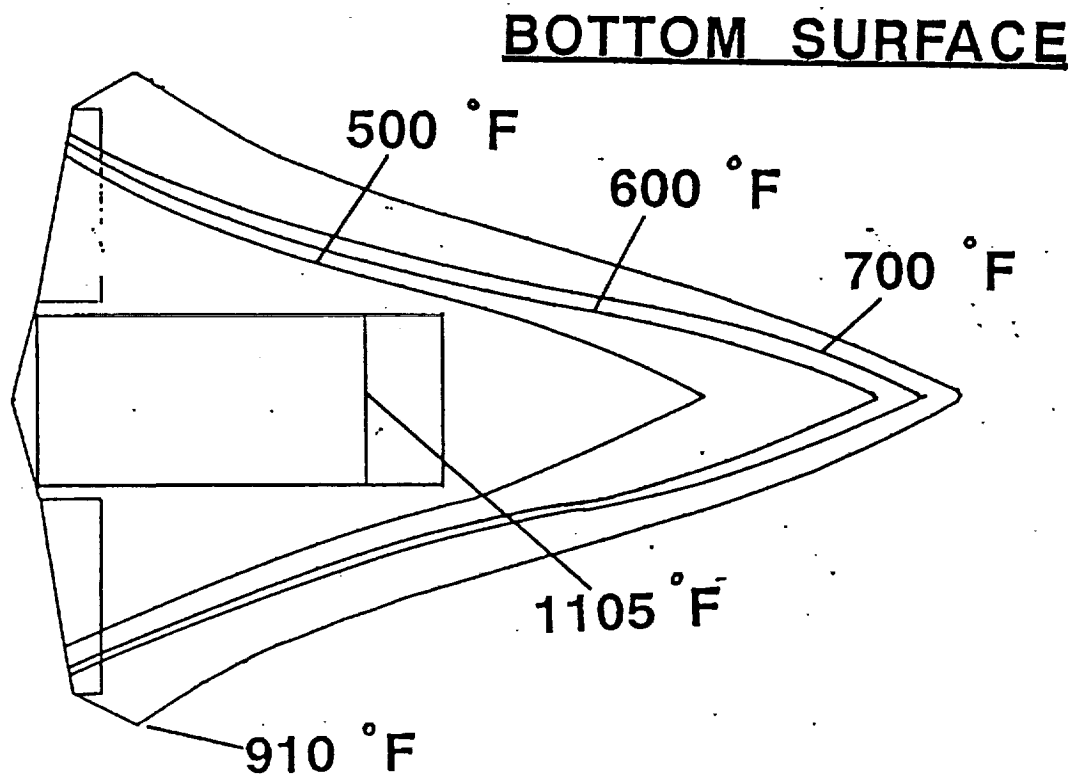
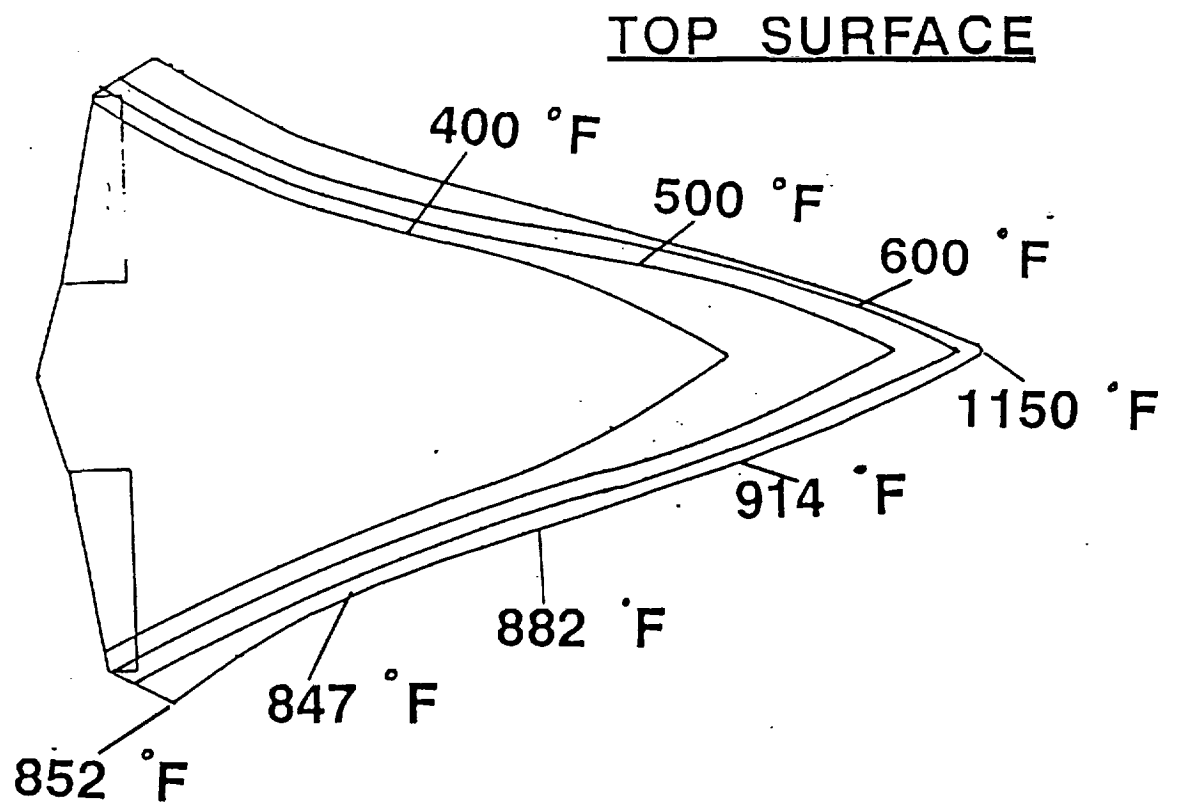


Figure 32. Temperature contours

changes. As you can see, the temperature grid lines from the top surface are back much farther on the bottom surface. Finally, temperature along the leading edge drops as sweep angle decreases, but comes back up as sweep angle rises once again.

Many of the same principals used for the nose, and leading edge analysis were applied once again for the CTM. The additional theory used was a cone analysis made up of cylindrical and delta wing equations from CDHEAT. Temperatures were basically a function of geometry and how far back you go in a radial direction  $x$ .



## TEMPERATURE DISTRIBUTION

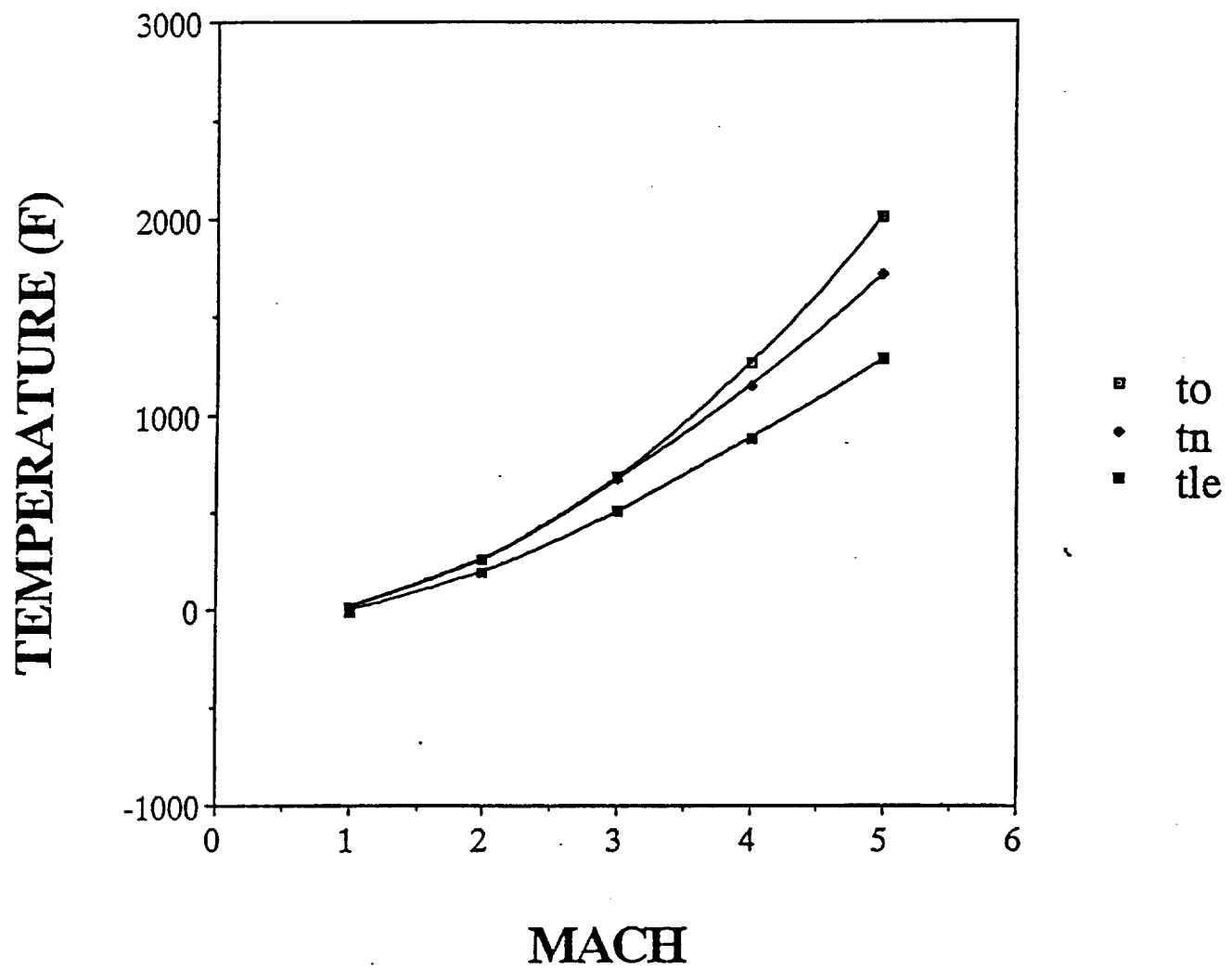


Figure 33. Temperature distribution across flight regime

## STABILITY AND CONTROL ANALYSIS

The stability of this waverider was analyzed for longitudinal static and dynamic stability. A positive static margin is a result of the center of gravity (cg) of the aircraft being in front of the aerodynamic center (ac) of the aircraft. The heaviest component as well as the densest component of this plane is the JP fuel. The fuel is located in the rear of the airplane, putting the cg, with full fuel, at 52.9 feet from the nose. The ac is located at approximately 46.7 feet from the nose. This calculates to a static margin of  $-.176$ , an unstable aircraft. Even with the fuel tanks empty, the triangular shape of the waverider alone leads to a rearward cg located at 49.0 feet from the nose. This static margin is also unstable at  $-.066$ . Both of the cg's are located 1 foot above the bottom of the center of the plane in the vertical plane.

An unstable aircraft is helpful at takeoff and during maneuvers, using less control surface area to rotate the aircraft upwards. Also, a control system will be used to make the aircraft stable during flight.

The longitudinal dynamic stability was analyzed by using known dimensions and aerodynamic characteristics with a standard linearized theory. The most obvious stability derivative which is of interest is  $M_w$ . The value for  $M_w$  is  $.0039$ . This is a function of the static margin and would be negative, like most stability derivatives, if this aircraft was stable. Also, the characteristic polynomial for

longitudinal analysis has sign changes which indicate an unstable aircraft.

The control system will use simple control loops using the stability derivatives with design constants to change the stability characteristics of the aircraft, making it stable during flight.

The control surfaces selected were conventional. A low-aspect-ratio twin tail is used. These tails were chosen to help keep the aircraft from entering a flat spin or unstable yawing. Each tail surface has a planform area of 25 square feet. Each vertical tail rotates as an entire rudder, allowing latitudinal control of a one-engine out condition. The elevators-aileron-flaps are built into single flaps near the rear wingtips of the waverider. They have a planform area of 30 square feet with an aspect ratio of 6.3 each. Each flap has complete independent controls to perform their several functions such as: flaps for takeoff, elevators for flight controls, and ailerons for roll control.

# Static Stability

$$U_0 = 3870 \text{ ft/sec}$$

$$\begin{aligned} \text{Static Margin} &= -.066 \text{ (empty)} \\ &= -.171 \text{ (full)} \end{aligned}$$

## Stability Derivatives

$$\begin{aligned} X_u &= -.0019/\text{sec} & Z_u &= -.013/\text{sec} \\ X_w &= -.38/\text{sec} & Z_w &= -.055/\text{sec} \\ M_w &= .0039\text{sec/ft} & M_q &= -.01/\text{sec} \\ M_{\partial e} &= -.216/\text{sec} & Z_{\partial e} &= 6.75/\text{sec} \end{aligned}$$

Figure 34. Stability derivatives

## Longitudinal State Equation

$$\begin{bmatrix} \dot{u} \\ \dot{w} \\ \dot{q} \\ \dot{\partial} \end{bmatrix} = \begin{bmatrix} -.0019 & -.38 & 0 & -32.2 \\ -.013 & -.055 & 3872 & 0 \\ 0 & .0039 & -.01 & 0 \\ 0 & 0 & 1 & 0 \end{bmatrix} \begin{bmatrix} u \\ w \\ q \\ \partial \end{bmatrix} + \begin{bmatrix} 0 \\ 6.75 \\ -.216 \\ 0 \end{bmatrix} \begin{bmatrix} \partial e \end{bmatrix}$$

## Pitch Rate Dynamics

$$\frac{w(s)}{\Delta(s)} = \frac{6.75s^3 - 836s^2 + 1.59s - .09}{s^4 + .67s^3 - 13.2s^2 - .0287s - .0016}$$

Figure 35. Longitudinal state equations

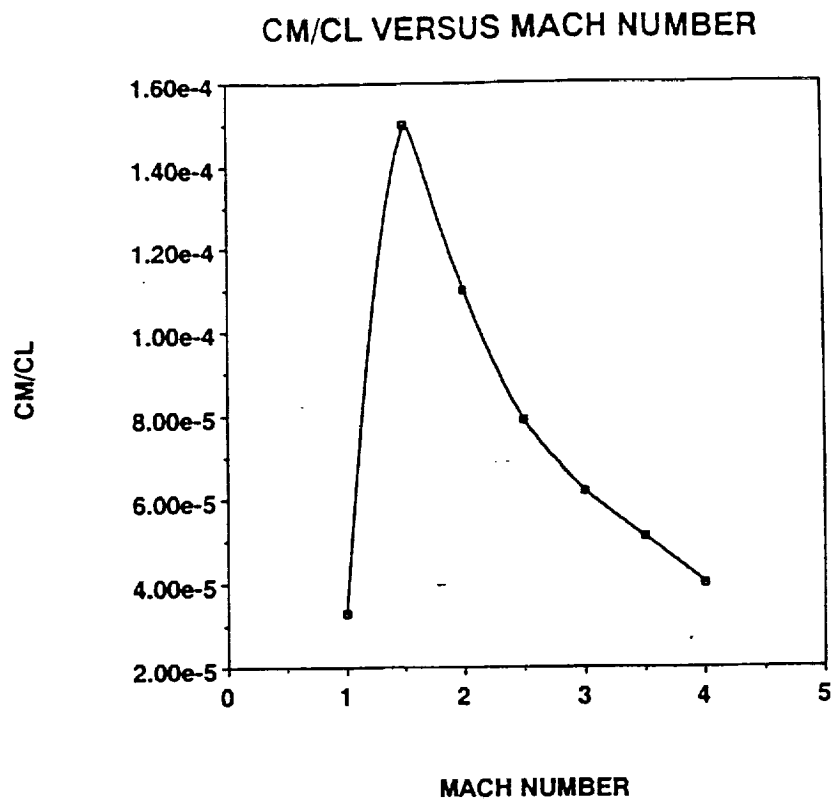


Figure 36.  $C_m/C_l$  versus Mach number

## Control Loop

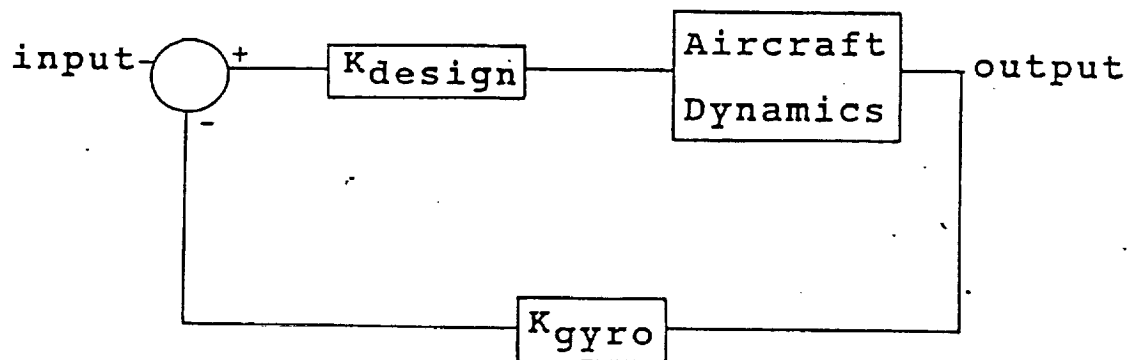


Figure 37. Simple stability control loop

## LANDING GEAR

The aircraft carrier environment has placed many special requirements on the design in general. The design of landing gear for this aircraft is also influenced by the carrier environment.

Navy specifications are summarized in figure . The tip over angle and maximum angle of attack requirements determine the location and height of the landing gear. These values are checked by calculating the static gear loads for the main and nose gears and confirming these loads are correctly distributed with respect to braking and steering. By iterating between the angle and steering/braking requirements the best gear position was found to be following:

	Distance from nose	Distance from Center
NOSE GEAR	15 feet	0 feet
MAIN GEAR	59 feet	15 feet

Landing loads were determined based on the required 22 feet per second sink rate for carrier landings. The landing loads determined shock absorber stroke length and diameter on the main gear.

The landing, braking and static loads all combined to select a suitable tire system. The main gear uses 30" x 7.7" tires inflated to 220 psi. The nose gear uses 26" x 7.5" chined tires inflated to 180 psi.

Figure and figure show the basic gear design. The main gear retract toward the center line, while the front gear retract to

the rear due to the volume constraints of the waverider.

## AIRCRAFT LANDING GEAR DESIGN

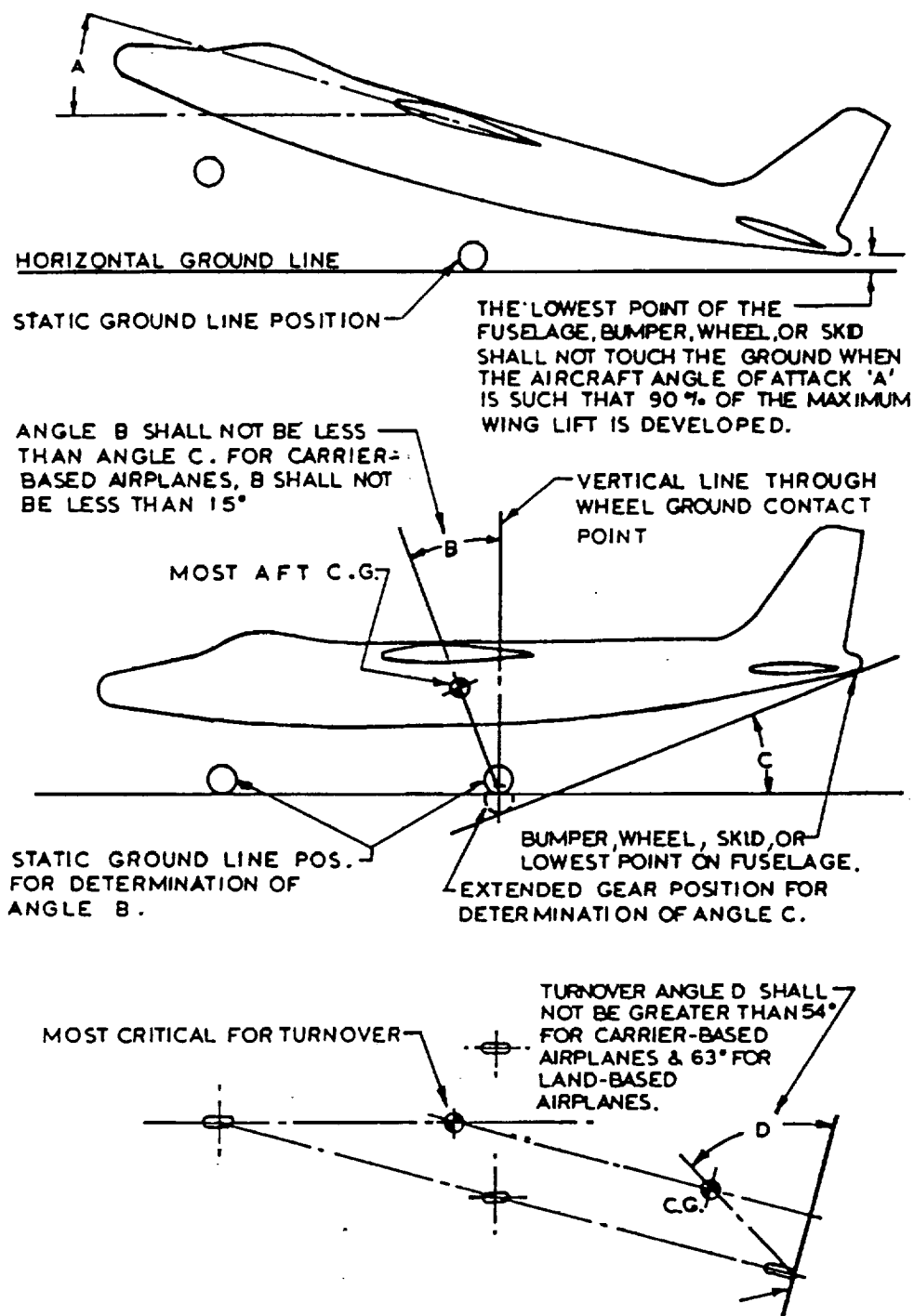
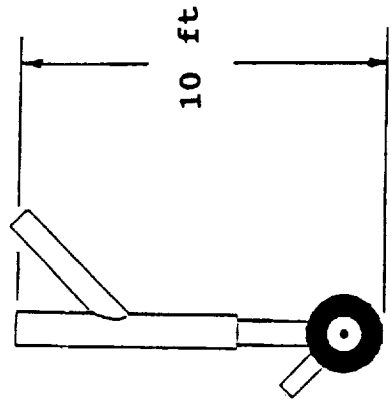


Figure 38. U.S. Navy landing gear requirements



# FRONT GEAR



# MAIN GEAR

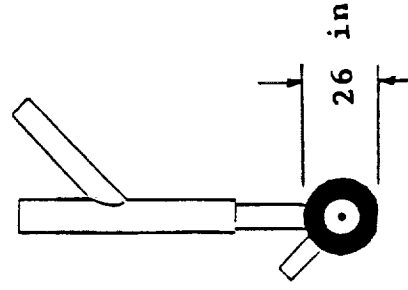
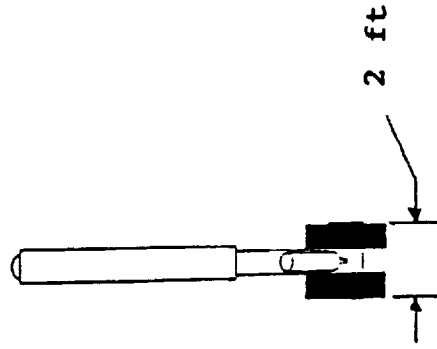
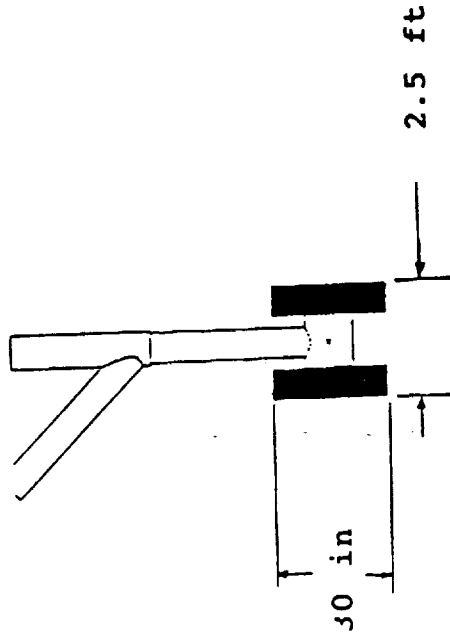
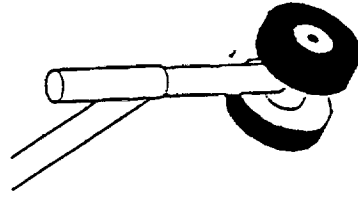
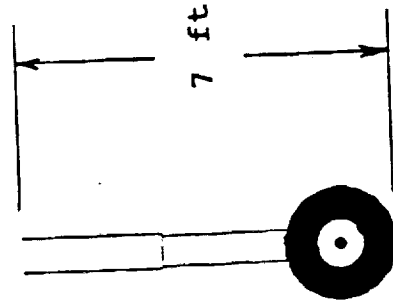


Figure 39. Main landing gear

Figure 40. landing gear

# LANDING GEAR SPECIFICATIONS

## MAIN GEAR

HEIGHT	7 FEET
DIAMETER	8 INCHES
STROKE	2.5 FEET
TIRES	30" X 7.7"

## NOSE GEAR

HEIGHT	10 FEET
DIAMETER	6 INCHES
TIRES	26" X 7.5"

Figure 41. Gear specifications

## COST ANALYSIS

In the context of current military downsizing and budget cuts, projects such as the one studied above must prove their usefulness will outweigh their cost. Thus, predicting the production and operating costs in this phase of design, while difficult, is important in determining the feasibility of a design.

In determining the production costs for this design, the method detailed in Fundamentals of Aircraft Design by Leland Nicolai was used to determine the engineering, tooling, manufacturing, and quality control hours required. Labor costs per hour were based on "wrap rates". The wrap rate incorporates all costs of labor such as insurance, benefits, and salary into an hourly cost. This allows the predicted costs to accurately reflect the total costs of labor. The Nicolai method was also used in predicting the costs of materials, development support, and flight test operations.

The costs shown in figure are for development, flight test and production. They are based on the production of twelve aircraft with the first two production aircraft serving as test aircraft in order to lower costs.

Operational costs are shown in figure. No standard list of the costs incurred by an operational reconnaissance aircraft could be found. Thus, fuel, materials, and maintenance were taken to be the extent of operational costs for this design. The costs are based on 90 missions of three hours per year. Maintenance man hours per flight hour were

# **COST ANALYSIS**

## **DEVELOPMENT & FLIGHT TEST**

FLIGHT TEST OPERATIONS	\$ 120,000,000
DEVELOPMENT SUPPORT	1,820,000,000

## **PRODUCTION**

ENGINES & AVIONICS	\$ 210,000,000
MANUFACTURING LABOR	783,900,000
MATERIALS & EQUIPMENT	407,100,000
AIRFRAME ENGINEERING	3,480,000,000
TOOLING	1,220,000,000
QUALITY CONTROL	<u>112,800,000</u>

TOTAL \$ 8,153,000,000

BASED ON 12 AIRCRAFT = \$ 680,000,000/AIRCRAFT

Figure 42. Cost breakdown

## **OPERATIONAL ANALYSIS**

MAINTENANCE	\$ 12,000,000
MATERIALS	14,000,000
FUEL	6,000,000
TOTAL	\$ 32,000,000

Figure 43. Operational costs

estimated at 300 with a wrap rate of 150 dollars per hour. Fuel costs were estimated at \$1.75 per gallon of JP-X with 9300 gallons used per flight. The materials costs were scaled from other carrier based aircraft based on the aircraft weight and the materials to maintenance cost ratio.

The resulting costs appear to be low when compared to those of the SR-71 (\$300 million/year). This is most likely due to the omitting of some phase of operating costs rather than underestimating of the costs considered.

## SUMMARY

After spending eighteen weeks for a conceptual design, many trade studies were performed to select the best possible configuration for an aircraft to meet the Scarlet II project requirement. The first consideration that was given when designing this aircraft is that it must first meet the requirements of which applies to any naval carrier based aircraft. These requirements were in both size and weight. This aircraft was not to exceed eighty feet in length, seventy-five feet in wingspan, 100,000 pounds in take-off weight, and 80,000 pounds in empty weight.

After studying several configurations from AIREZ and other NASA reports on hypersonic aircraft, a waverider from MAXWARP was chosen for its high lift-to-drag ratio, which translated into an excellent cruise aircraft. To power this aircraft, a set of two augmented turbofan engines was chosen from a selection of augmented turbojets, combinations of turbofan/ramjets and integrated ramjets, because efficient powered flight was required for speed ranging from zero to Mach 4.

Using the waverider and turbofan engines as leads, weight analysis was performed using HASA software and thermal protection was analyzed with the aid of CD-HEAT software. Other analysis included trajectory, landing gear and cost.

## CONCLUSION

After eighteen weeks of research, this conceptual design is for a hypersonic reconnaissance aircraft that is to operate on board of an aircraft carrier. This report has shown that a 6,000 nautical mile range naval hypersonic aircraft is very plausible. The configuration chosen was a waverider powered by two augmented turbofan engines burning JP fuel. JP fuel, which can be stored at room temperature for long period of time would not present any difficulties aboard a carrier.

A typical mission would be to take-off from an aircraft carrier with the aid of a catapult, climb to 80,000 feet following a "constant q" trajectory with a level flight near sonic speed, cruise 6,000 nautical miles at Mach 4, descent, and land back on the same aircraft carrier. This mission would require roughly 2.7 hours.

## REFERENCES

1. AIREZ (preliminary aerodynamic design program developed by Bud Zeck, Boeing Aircraft Company).
2. MAXWARP (Maryland Axisymmetrical Waverider Program), developed at the University of Maryland by Corda, Bowcutt, and Anderson.
3. Nielson, Jack N., Hesh, Michal J., "Tactical Missles Aerodynamics", Chapter IV, "Waveriders", Schindler, L.H., Naval Surface Weapons Center, Silver Springs, Maryland.
4. Ibid.
5. Hoerner, Sighard F., "Fluid Dynamic Lift", Hoerner Fluid Dynamics, Bricktown, N.J., 1975.
6. Miele, Angelo., "Flight Mechanics Volume 1, Theory of Flight Paths," Addison Wesley Publishing Company, Inc., 1962.
7. Raymer, Daniel P., "Aircraft Design: A Conceptual Approach", American Institute of Aeronuatics and Astronautics, Inc., 1989.
8. Nicolai, L.M., "Fundamentals of Aircraft Design", METS Inc., San Jose, 1984.
9. HASA (Hypersonic Aerospace Sizing Analysis for the Preliminary Design of Aerospace Vehicles, by Gary Harloff and Brian M. Berkowitz).